A PHOTO-ELASTIC ANALYSIS OF LADLE HOOK DESIGN THEORY

by

Rudolf Harold Thielemann

A THESIS

submitted to the

OREGON STATE AGRICULTURAL COLLEGE

in partial fulfillment of
the requirements for the
degree of

MASTER OF SCIENCE

June 1936

APPROVED:

[redacted]

In Charge of Major-Professor of Mechanical Engineering and Head of the Department

[redacted]

Chairman of School Graduate Committee

[redacted]

Chairman of College Graduate Council

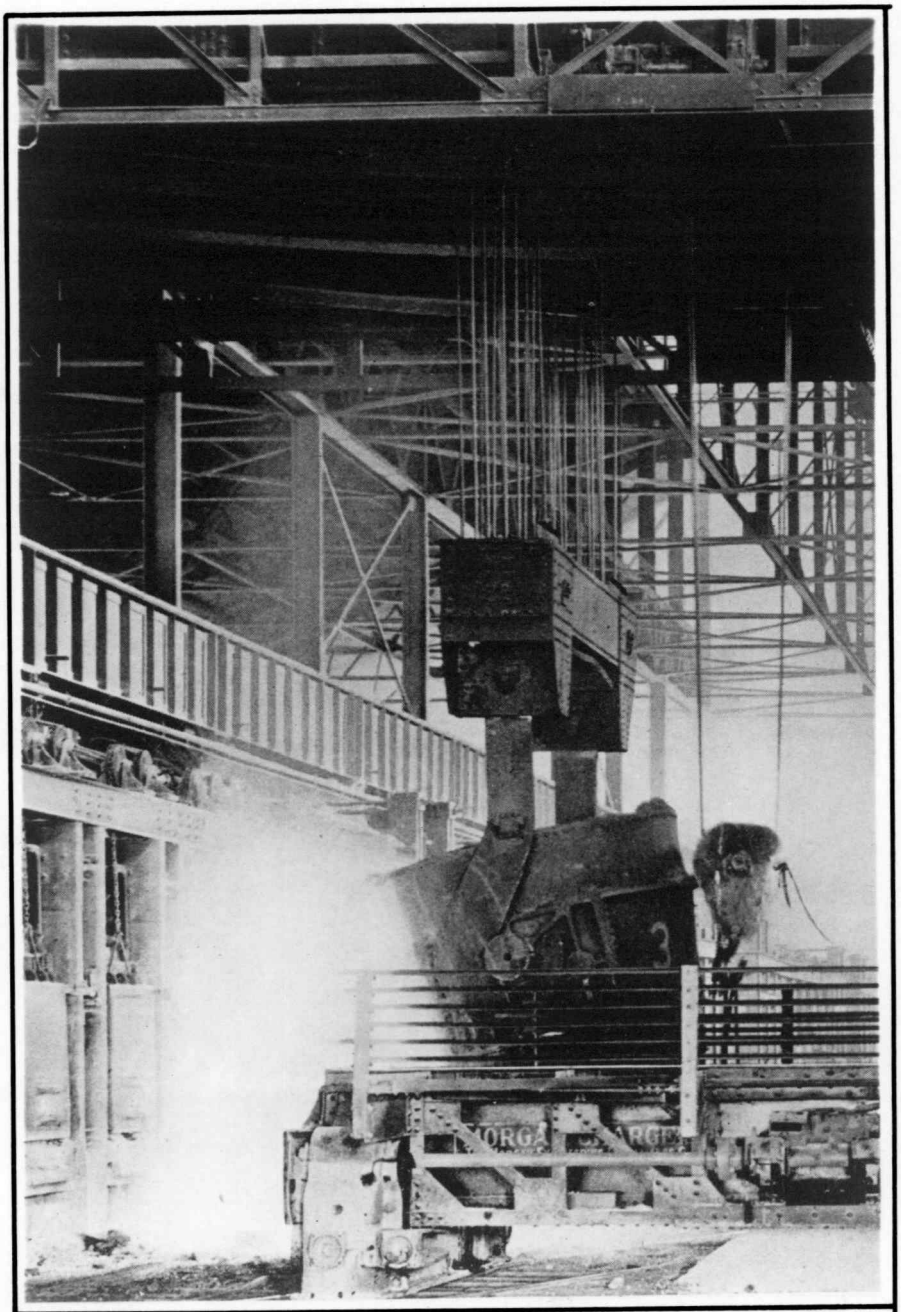

Frontispiece.-Morgan 125-Ton Ladle Crane as Used in the Steel Industry

ACKNOWLEDGEMENTS

The suggestion for this investigation came through Mr. W. H. Ball, assistant chief engineer of the Morgan Engineering Company located in Alliance, Ohio, and manufacturers of large ladle hooks as used in the steel industry. Since the ladle hooks are manufactured from a laminated design, the steel plates being held together by rivets, it was thought that probably a photo-elastic investigation of the same might give valuable information as to the best location of the rivet holes and on hook design theory in general. Great appreciation is due the Morgan Engineering Company for their cooperation in supplying detail drawings of ladle hooks as manufactured by them and for other information supplied by them in connection with hook design theory.

Thanks and credit are due Mr. H. D. Eberhart of the U.S. Engineer Office in Portland for his assistance and interest in the work, and for the use of two of his diagrams on photo-elastic theory as used in his thesis of last year.

Deepest appreciation is extended Professor S. H. Graf, Head of the Department of Mechanical Engineering, for his cooperative and constructive ideas in connection with the problem and also for his assistance in planning and performing many of the tests.

R.H.T.

TABLE OF CONTENTS

TABLE OF ILLUSTRATIONS

FIGURES

TABLES

PART I

INTRODUCTION

A PHOTO-ELASTIC ANALYSIS OF LADLE HOOK DESIGN THEORY

PART I. INTRODUCTION

1. STATUS OF THEORY OF CURVED BEAMS. Since curved beams comprise such important machine elements as crane hooks and punch frames, the nature of the distribution of stresses in a curved beam has long been a subject of investigation. Much laboratory work has been conducted in which both models and full size specimens have been tested and their deformations measured by the use of the strain gage or some other means of measuring dimensional changes to a high degree of accuracy. Other investigations have been made using elastic membrane analogies for the determination of stresses and in some instances the use of the polarized light method, photo-elasticity, has been applied. Very few results seem to be available, however, from the latter investigations mentioned.

From the results of these investigations, authors have proposed various derived equations to determine the stresses for the particular problem studied but from an interpretation of the available results published it appears that no one equation will hold for every condition involved in the curved beam. Also, in studies where stresses were determined from measurements of strain, or displacements, approximations had to be made as to the elastic constants of the material used and also because of errors that exist

in measuring circumferential strains on a chord instead of on a circumferential arc.

Up to the present time, three leading theories have been advanced to express the distribution of stresses in curved beams subjected to bending. The three mathematical formulas, appearing in several publications, need not be repeated in detail. (14). It is essential here simply to note the general principles and hypothesis underlying each theory, as follows:

1. The ordinary beam theory assumes that in a cross-section of a curved beam the stresses due to bending are distributed according to the same law as in the case of a straight beam.

2. The Winkler-Bach theory takes account of curvature and is based on the hypothesis that plane transverse sections remain plane after loading.

3. The Andrews-Pearson theory, proposed as a refinement of the Winkler-Bach theory, takes account of the additional consideration that the radial dimensions of the cross section after loading are changed by the Poisson-ratio effect of transverse strains resulting from normal stresses.

It should also be noted that both the Winkler-Bach and the Andrews-Pearson theory, to reduce complexity, confine consideration to the plane of maximum moment normal to the direction of loading. On this plane the resultant external shear is zero and it is assumed that internal shearing

Numbers in parenthesis refer to bibliography.

stresses on this plane may be neglected without appreciable error.

2. Conditions of the Problem. This investigation, in particular, has to do with the study of the distribution of stresses in two ladle hooks, the particular designs being furnished by Mr. W. H. Ball, assistant chief engineer of the Morgan Engineering Company located in Alliance, Ohio. These hooks are of a rectangular cross section and of a laminated construction, the individual plates being held together by the use of rivets. The capacity of the hooks is sixty-two and one half tons each. Figure 15 shows a detailed drawing of the two hooks studied.

The purposes of this investigation were as follows:

(a) To investigate the adaptability of the photo-elastic method to curved beam analysis with particular reference to the design of large ladle hooks.

(b) To analyze, as far as possible, the stresses through the section of maximum moment of the particular ladle hook designs as proposed.

(c) To determine, as far as possible, the effects of the rivet holes, as located in the designs studied, on the stress concentrations that might exist in the stressed sections.

(d) To inquire as to the correlation and adaptability of accepted hook design theory with photo-elastic determinations.

3. Stress Analysis in General. To the designing engineer the problem of determining the critical unit stress to which any material in use in a machine or in a structure may be subjected is of great importance. By critical stress is meant that stress which will cause the machine or structure to be no longer capable of performing the function for which it was designed.

Stress analysis, therefore, is only one of three factors that make for an ultimately successful performance. In the first place, the loads or forces acting must be known; second, the stresses produced by these loads or forces must be determined; and third, the knowledge of the materials concerned must be sufficient to insure the product to be both safe and economical. An error in any one of these may cause either failure or gross extravagance. Since both are wasteful, it is customary to strive for the middle ground of efficiency and economy.

In the present problem, the design, the loads to be used, and the material that would be the most suitable both as to manufacture and performance were known, leaving only the particulars of stress distribution resulting from these known factors to be determined.

When a load or force is applied to an elastic material, it resists any attempt to change its size or shape. The customary way to measure the intensity of the deforming force is in units of force or weight acting over an

area, as pounds per square inch. This intensity of force being resisted by a material is known as stress, and may be applied to a point as well as to a finite area. Quantities of this sort defy direct measurement. There is no scale or mechanism known to measure pounds per square inch. For this reason resort must be made to indirect methods, by measuring either those things that cause the stress along with the dimensions of the stressed area, or by measuring the results of that stress acting in the form of strain, displacement, or other changed properties, and finally by using these quantities to compute the stress.

First and foremost among the methods of stress analysis must be placed that of mathematical solution. This includes both the fundamental theories of statics and ordinary formulas as well as the more exact elastic theory. All of these expressions are based on the assumption that there is continuity of elastic action throughout the members and therefore that the stress distribution on any section can be expressed by some mathematical law or equation. An example of this is the tension member in which the stress is assumed to be uniformly distributed over each cross section. Another is a beam in which the stress increases directly as the distance from the neutral axis.

But the assumption that there are no discontinuities in the stress distribution may be erroneous and the results obtained not even a rough approximation of the real stress

at a point. Some conditions that cause discontinuities and stress concentrations are; abrupt changes in section; discontinuities in the material itself, as voids in concrete, pitch pockets and knots in timber; initial stresses in a member due to shrinking, setting, heat treatment, or cold working; and excessive pressures at points where external loads are applied. Stresses due to actions such as these are termed localized stresses and sometimes prove to be the controlling factor.

Problems of this kind must be dealt with and since the mathematical solution is either too limited or becomes too involved other methods have had to be developed. Some of these are very ingenious and unique for certain kinds of problems, and as a brief review, they will be mentioned here.

Special properties of brittle, ductile, or plastic material have been used to determine stresses in elastic material. (16)

Another group, and perhaps the most common, depends upon the use of scale models where, in general, the model and the prototype have essentially the same form. The extent of the similarity must in all cases be based upon a strict dimensional analysis. This often leads to unsurmountable difficulties, particularly where constants of gravitational acceleration, elasticity, etc., must be reduced or increased to conform with the requirements of dimensional homogeneity between the model and the prototype.

Problems in indeterminate structures have been solved by the use of dynamically similar models where deflections could be measured and the resulting stresses computed.

Still another group depends upon the similarity of the differential equations describing elastic, electric, hydrodynamic, and thermodynamic phenomena. These are commonly termed analogies. Seldom do the analogous systems have even the slightest physical resemblance.

It is of importance that a great number of problems in stress analysis are completely independent of the elastic constants and in many cases the prototype and model are geometrically similar in all respects. For this reason, no concern need be given to the generally present possibility of variation of linear scales and physical constants in the prototype and in the model. The photo-elastic method of stress analysis is one which owes a great deal to this independence for its simplicity, and because it is so conveniently applicable to many investigations of stress distribution, it has been singled out for an extended discussion.

4. Photo-elasticity in the Field of Stress Analysis. Photo-elasticity may be defined as the science of measuring stress by utilizing the effect of the changed properties of the material itself on the transmission of light. The principles of the method are not new, for as early as 1816 Sir David Brewster discovered that poorly annealed

or heavily compressed bits of glass displayed properties of double refraction when observed in a beam of polarized light. The possibilities of employing this phenomenon as a tool in the study of stress analysis were at once apparent to Brewster, but it was not until many years later that the problem of interpreting the interference color bands in terms of stress was solved. About 1850 the renowned mathematician, James Clark Maxwell developed a theory which indicated that three groups of data were sufficient for the complete determination of the magnitudes and directions of principal stresses at any point in a specimen. Unfortunately, Maxwell's equations involved certain complicated functions and curvature relationships which made accurate numerical solutions practically impossible. It was not until 1913 when Professor A. Mesnager of Paris made what was probably the first serious attempt to apply the photo-elastic method of analysis to an engineering problem when by this method he studied stresses in a glass model of a proposed reinforced concrete bridge which was to be built across the Rhone.

Until recently, progress was held back because of the fact that glass was the only material used; it is hard to machine and likely to contain initial stresses. Professor E. B. Coker (5), of Cambridge, discovered that other transparent isotropic substances such as celluloid and bakelite also became doubly refracting when strained

by external loading. About the same time Professor L. N. G. Filon, also of cambridge, simplified Maxwell's method of stress determinations from optical observations. It is due, mainly, to these two men that photo-elastic science has advanced until today the method is being acknowledged as a powerful tool in the field of coplanar stress analysis.

5. Advantages and Limitations of Photo-elasticity. Photo-elasticity, like all other methods of stress analysis in use today, has its advantages and limitations. First, it is satisfactorily applicable only to coplanar stress problems, i.e., problems in which the loads and stresses lie in the same plane. However, since a great many problems fall into the one or two coordinate class, this limitation to the method is not as serious as one might at first suspect. Many problems in three dimensions may be broken up and analyzed as coplanar systems.

Until recently, the cost of prisms for producing polarized light has made photo-elastic equipment quite expensive. However, in the last year a new material in the form of a screen glass has been invented by Mr. Edwin Land and is being manufactured under the trade name "Polaroid". This new glass is much less expensive than the Nicol prisms or other light polarizing equipment and in addition has the advantage of being able to more completely polarize white light than do Nicol

prisms monochromatic light of the required wave length. With "Polaroid" screens it is possible to obtain a very large area of polarized light, making them very useful in connection with photo-elastic investigations.

There are many advantages of photo-elasticity as a method of stress analysis which are not common to other methods. Local stress concentrations, maximum shear at all points and the magnitude of the tangential stress along any unloaded boundary may be determined from direct observations. In addition, the magnitude of stress concentrations, the direction of the principal stresses, and the quantitative values of the principal stresses in many indeterminate structures can be obtained by either graphical or mathematical solutions. Methods for analyzing photo-elastic observations will be outlined later, but it is important to note that photo-elasticity is the only method by which a picture of stress distributions in a load member can truly be observed.

6. Conditions of Similarity. As previously mentioned, many problems in stress analysis are completely independent of the elastic constants. This is true of problems where the stress on the boundary is everywhere known. In treatises on elasticity (11:145)-(5:129) it is shown that the stresses in any two-dimensional problem may be expressed in terms of a function known as Airy's stress function. In itself, this function is completely indepen-

dent of the elastic constants of the material. For cases where the boundary conditions are all stress conditions, the stresses in terms of this stress function also do not involve the elastic constants and the distribution of the stress is entirely independent of the material used.

The same cannot be said, however, when the boundary condition involves either displacements or partial displacements (5:414). But as stress conditions can be substituted for these displacement conditions, the problem may still be solved.

By the photo-elastic method, then, it can be said that as long as the material of the model is isotropic, homogeneous, and obeys Hooke's law of proportionality of stress to strain, results from a model, of say bakelite, may be applied to usual engineering materials.

PART II

THEORY

PART II THEORY

1. Relationship of Principal Stresses and Shear.

Regardless of the kind of loading that may be applied to an elastic material, there are possible only three different kinds of stresses that may exist in that material, namely, tension, compression, and shear. These may be considered as acting in any direction and in any combination on the faces of a small element of the material. When the exterior forces are all in one plane, or coplanar, the stress normal to that plane is zero or at least negligible in a thin plate. With the remaining forces constant over any cross section the element of volume, the cube, may be thought of as a square with unit stresses acting on the four faces. Since this small square must be in equilibrium, the stresses on opposite sides, when resolved in one direction, will be equal and and opposite, and the square may be rotated so that all the stresses are perpendicular to the four sides. These normal stresses, acting on planes along which the shear is zero, are called principal stresses. They are the maximum and minimum acting at any point and are at right angles to each other. If they are known, the stresses in any direction may be obtained most conveniently in terms of normal and tangential components. This tangential component is called shear.

Because of the fact that some materials are weakest in shear, the maximum value of shear at any point is important. It is easily shown that this maximum value of shearing unit stress at a point in a stressed body is equal to one-half the algebraic difference of the maximum and minimum unit stresses.

Consider a small element AD, Fig.1, on the opposite faces of which the principal stresses P and Q are acting. A tensile force will be considered as positive and a compressive force as negative. If a plane is passed through a corner, B, it will make an angle θ with the side AB. Taking the triangle BAC as a free body, resolve all the forces parallel to the plane BC. Since P,Q, and the shear S, are all unit forces they must be multiplied by the area of the face on which they act. As the thickness is unity, this is equal to the length.

Therefore:

$$BC\ S = AB\ P \sin\theta - AC\ Q \cos\theta$$

or $$S = \frac{AB}{BC} P \sin\theta - \frac{AC}{BC} Q \cos\theta$$

but $$\frac{AB}{BC} = \cos\theta \quad \text{and} \quad \frac{AC}{BC} = \sin\theta$$

so that $$S = P \sin\theta \cos\theta - Q \cos\theta \sin\theta$$

and $$S = (P-Q) \sin\theta \cos\theta$$

or $$S = 1/2\ (P-Q) \sin 2\theta$$

The $\sin 2\theta$ is a maximum and equal to 1 when $2\theta = 90°$ or $\theta - 45°$. Therefore, the maximum shear is equal to 1/2 (P-Q) and acts in a direction making 45° with the prin-

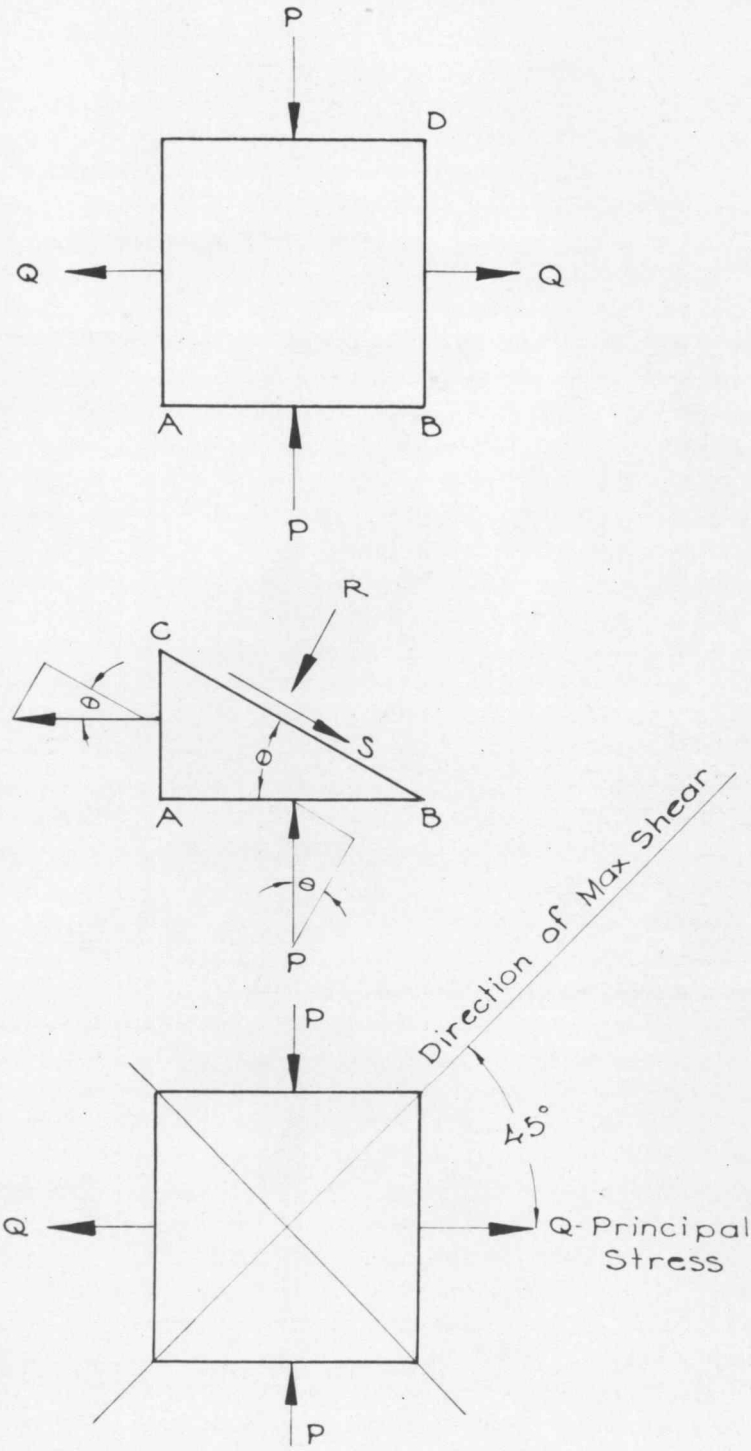

Fig.1.-Principal Stresses and Determination of Shear.

cipal stress.

2. General Theory of Photo-elasticity. The method of determining the magnitudes of stresses by matching colors of relative light retardations is very interesting. The external loading on the thin transparent plate is responsible for the existence of two principal stresses, usually designated P and Q, at every point within it. These principal stresses cause the plate to assume the property of double refraction, causing the impinging beam of plane polarized light to break up into two orthogonal beams vibrating in planes which contain the directions of P and Q as elements. Of no less importance is the fact that the two beams pass through the plate at varying velocities, each beam being retarded in direct proportion to the magnitudes of the two principal stresses. Upon these two properties of the emergent light beam is based the whole science of photo-elasticity.

Fig.2 shows a ray of plane polarized light, OA, from a polarizing prism passing perpendicularly through a loaded plate at a point where the principal stress directions are P and Q as shown. The ray, OA, is broken up into its two orthogonal components, OB and OC, parallel to P and Q. If the principal stresses at this point are not of equal magnitudes, the emergent rays will be out of phase, since a relative wave retardation will then exist. Because of its orientation, only the com-

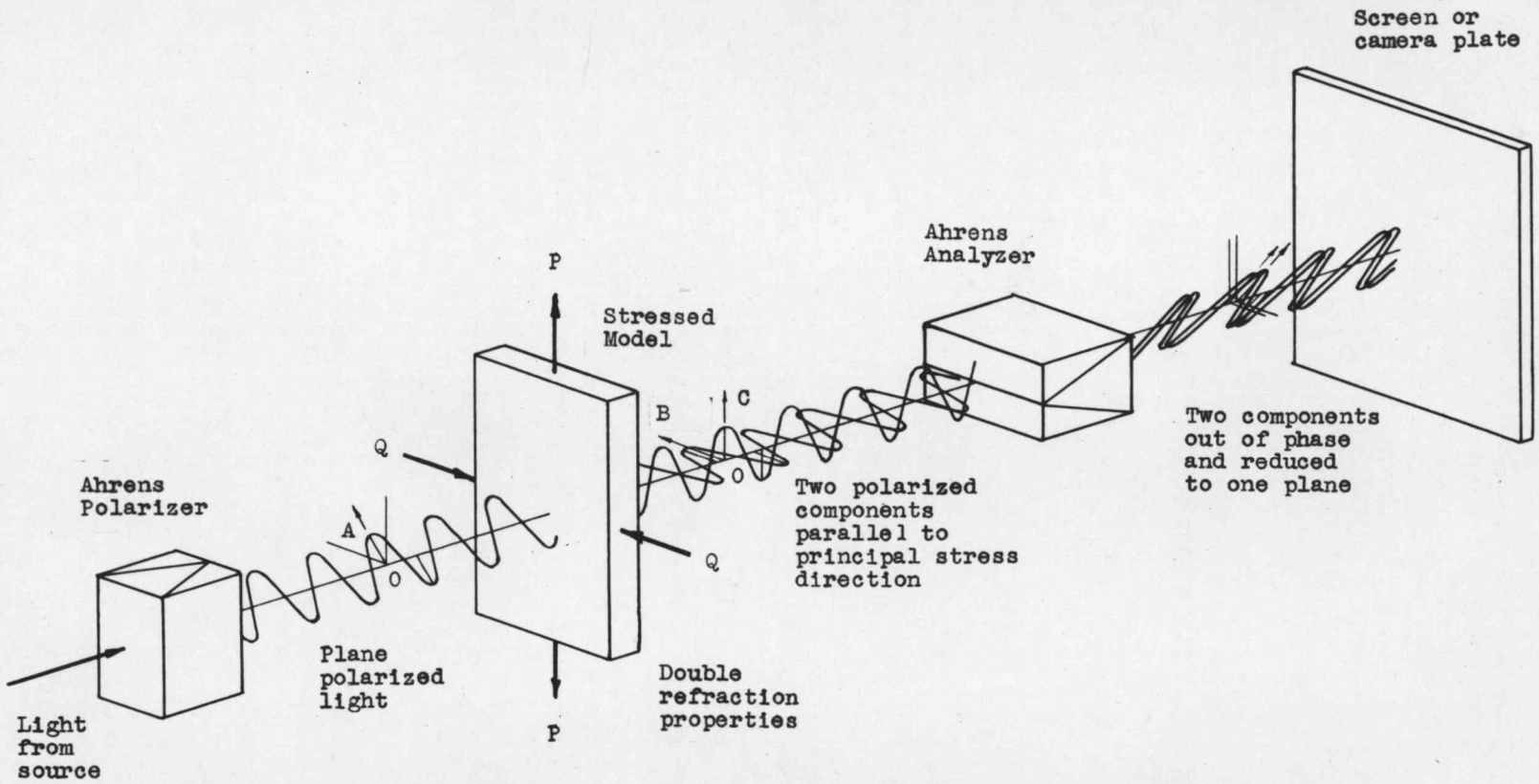

Fig.2.-Schematic Diagram of the Action of One Light Ray.

poments of the two beams which are parallel to a particular plane will be transmitted by the analyzer and the others will be absorbed. The light leaving the analyzer is also plane polarized, but is out of phase by the same amount as were the orthogonal beams that left the stressed point. The phase difference existing in the analyzed beam gives rise to the interference colors which appear to cover the surface of the strained specimen. Since the analyzed beam appears as an interference color and is dependent upon the phase produced by the unequal magnitudes of the principal stresses, it at once becomes apparent that these color bands are a direct measure of the difference of the principal stresses. Recalling that the maximum shearing stress appearing at any point is 1/2 (P-Q), it is found that a direct measure of the maximum shear is obtained.

Expanding the field of vision from the point O to an appreciable area of the stressed plate, a series of interference fringes or color bands will be noticed if a source of white polarized light is used. These color bands are called "isochromatics" and are the loci of points of equal maximum shearing stress or 1/2 (P-Q)= constant. Also, these isochromatic lines increase or decrease in a regular sequence so that the same color appearing several times will have a different value or a different "order". If a monochromatic light source

is used, interference causes a change of intensity so that light or dark bands or "fringes" are formed.

If at any point in the stressed plate the principal stresses are equal, regardless of their magnitudes, the relative retardation of the light waves will be zero and the two components emerging from the analyzer will be in phase, causing a dark point or line to appear. This black isochromatic then, means that at that point or line in the stressed plate P=Q and therefore $1/2\,(P-Q)$ = zero. Such a point at which the principal stresses are equal and the shearing stress is zero is termed an "isotropic" point.

So far, discussion has been only with the effect produced by the magnitudes of the principal stresses on a beam of polarized light. Considering now, that one of the principal stresses is in a direction that coincides with the plane of polarization, causing only one ray to emerge from the loaded plate: this ray will be in a plane that is at right angles to the plane of light that will be transmitted by the analyzing prism and therefore will be completely absorbed causing a dark band. This dark band is called an "isoclinic", since it is the locus of all points whose principal stress direction coincides with the plane of polarization. Fig. 4 shows isoclinic lines for one angular setting of the crossed prisms, the plane of polarization for

this setting being with the vertical. If a map is made showing the isoclinic lines for different positions of the plane of polarization, sufficient information will be obtained to develop a complete network of stress trajectories. (See Fig.20)

Referring to Fig.3, it will be noticed that a point exists in the loaded model lying in the plane of maximum moment about which the isochromatics or fringes occur as concentric bands. This point is an isotropic point, at which the shear is zero and the principal stresses are equal. Isotropic points are further characterized by the fact that isoclinics will always pass through them regardless of the angular position of the stressed plate with respect to the plane of polarization.

Using plane polarized light, then, a dark band may have either of two meanings; that the stress difference, (shear) is zero or that the stress direction coincides with the plane of polarization. To distinguish between the two, so called quarter-wave plates are inserted on each side of the stressed plate. The first quarter-wave plate has the power to circularly polarize light, that is, it produces an effect equivalent to spinning the beam of plane polarized light about its axis of propagation. When this light strikes the specimen it will have no directional properties capable of producing isoclinics. The second quarter-wave plate stops the

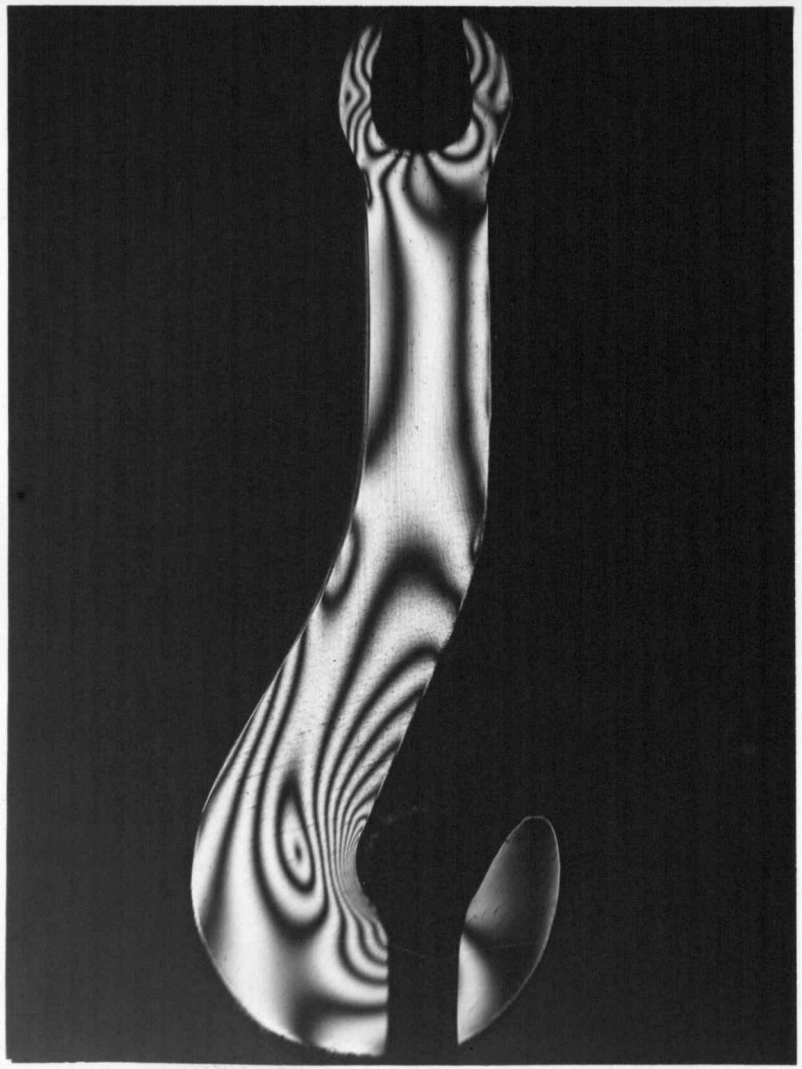

Fig.3.-Quarter-wave Plates in Place
Showing Fringes Only

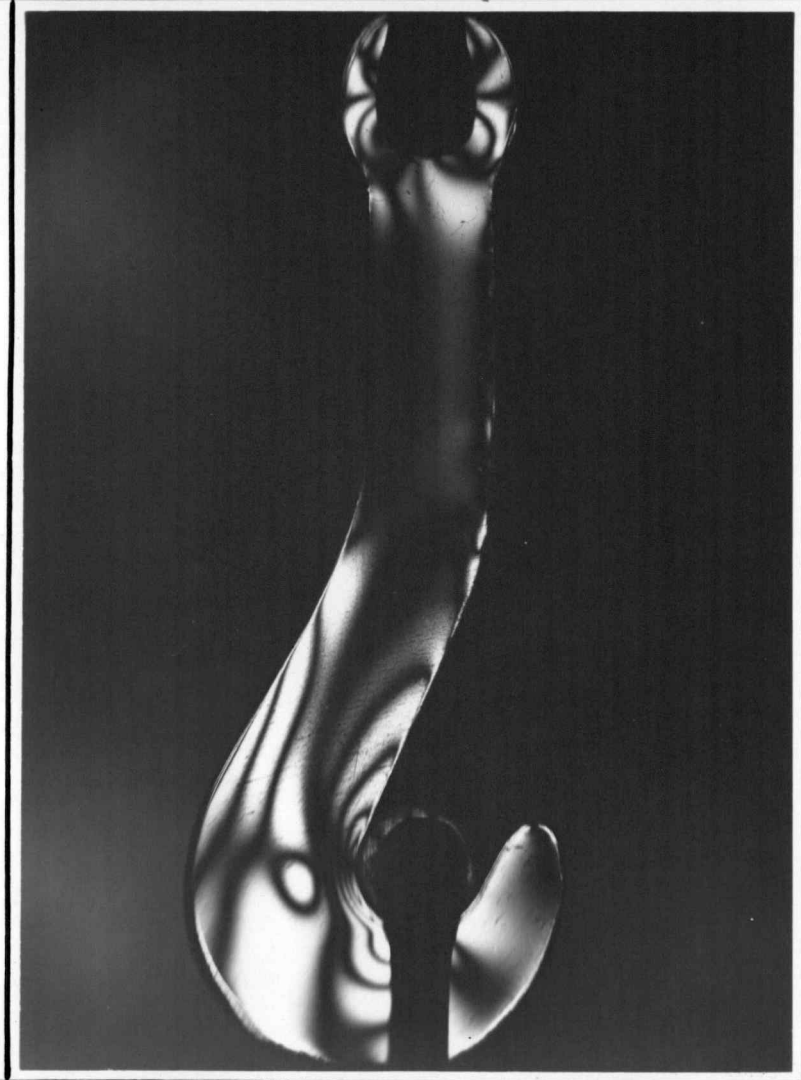

Fig.4.-Quarter-wave Plates Removed
Showing Fringes and Isoclinics

spinning of the beam so that, as before, only double refracted plane polarized light will strike the analyzer. With the quarter-wave plates in place, then, any dark band that is present can mean only that the stress difference at the point is zero. Since all the isoclinics are removed an uninterrupted view is obtained of the isochromatics, whether they are colored or are black. However, if the quarter-wave plates are removed and the two prisms are rotated simultaneously, the isoclinics will rotate and the isochromatics (P-Q) lines will remain stationary.

Quarter-wave plates are usually made from sheets of selenite or mica, split and accurately polished to a very definite thickness dependent upon the wave length of the light they are to circularly polarize. When white or polychromatic light composed of vibrations of different wave lengths is used, all the wave lengths except one will be eliptically polarized, giving somewhat undesirable directional properties. For this reason, filters are used to give a monochromatic source of the desired wave length, giving light and dark fringes instead of color bands and in addition making it possible to obtain much clearer photographs.

Knowing, now, that fringes represent lines of constant maximum shear (P-Q), it remains to determine or to calibrate the value of the fringes. The most satis-

factory method of determining the magnitude of the fringe or color order, in pounds per square inch, is to put a known load on a specimen in such a way that one of the principal stresses is zero and the other may be calculated using the common engineering formulas. A simple tension member in which the stress is all uniform and longitudinal is often used. The amount of stress required to change the color through a complete cycle is the fringe order. Perhaps the best method, however, is to use a simple beam with equal loads applied at points equidistant from the ends so that no vertical shear is present between the loads and the fringe magnitude increases from the neutral axis to the outside fiber. (Fig.11). As the transverse stress is zero, the color bands represent directly the longitudinal fiber stress which may be calculated knowing the bending moment applied and the dimensions of the beam. Because it calibrates the fringe orders in models under test in pounds per square inch, this is commonly known as a calibration beam.

For the purpose of clarity, the following statements will serve as a summary concerning the interpretation of information obtained optically from polarized light.

Color bands are isochromatics or fringes which are lines of constant shear or (P-Q) throughout the model.

Isoclinics are the loci of all points at which the

principal stress coincides with the plane of polarization or makes a constant angle with a reference axis.

Stress concentrations are indicated by the distance between isochromatics which is very small for large concentrations.

At unloaded boundaries or other places where one principal stress is known to be zero, the isochromatic is a direct measure of the other principal stress.

3. Determination of P and Q Separately. There are several methods that have been developed for determining the values of P and Q for the many different conditions that might exist, but since the graphical integration method was employed in this report, other methods will only be mentioned.

A. Method of Graphical Integration.

This method was developed by L. N. G. Filon and is derived in his book "Photo-elasticity" (5), in an article written by him in "Engineering" in 1923, and in other articles to which reference is made. (8),(13). There are modifications to the method and very often the problem being investigated presents a peculiar condition which can be more expiditiously treated by some variation in Filon's method. However, no attempt will be made to do any more than give Filon's method of analysis in its original form.

It has already been shown that the relative retarda-

tion from the stressed plate can be expressed as:

$$R = KT\ (P-Q) \tag{1}$$

This equation, in effect, gives a measure of the color band. It is also possible to express the shape of the curve as some function of two orthogonal coordinates, such as x and y, which lie in the plane of the model.

$$f(xy) = KT\ (P-Q) \tag{2}$$

where K = an optical constant

T = a constant proportional to the thickness of the model.

Similarly, the isoclinics can be expressed as another function,

$$f(xy) = \tan \phi = dy/dx. \tag{3}$$

where ϕ = the angle the plane of polarization makes with the X axis of the specimen.

Then, at any point in the model, such as A in Fig. 5, the following equilibrium equations hold:

$$\frac{\partial P}{\partial S_1} + \frac{(P-Q)}{\rho_2} = 0 \tag{4}$$

$$\frac{\partial Q}{\partial S_2} \quad \frac{(P-Q)}{\rho_1} = 0 \tag{5}$$

where P and Q are the principal stresses at A

S_1 and S_2 are the P and Q stress trajectories.

ρ_1 and ρ_2 are the radii of curvature of S_1 and S_2, taken as plus when the tangent to the curve rotates in a counterclockwise direction as following the curve in the general sense of the positive X or Y axis.

It is to be noted that these two equations are independent of all elastic constants; therefore the equations will hold regardless of the material being tested.

If the state of stress at some point is known and is expressed by P_o and Q_o, at an unloaded boundary, it is possible to determine stresses at points on the stress trajectories, such as A and B, Fig.5, by integrating equations 4 and 5. We thus have for the magnitudes of the stresses

$$P_A = P_0 - \int_0^A \frac{(P-Q)}{\rho_2} \, ds_1 \qquad 6$$

$$Q_B = Q_0 - \int_0^B \frac{(P-Q)}{\rho_1} \, ds_2 \qquad 7$$

These equations are in the form of line integrals whose paths of integration are the respective lines of principal stress.

The entire problem of determining actual numerical values for stresses by the photo-elastic method

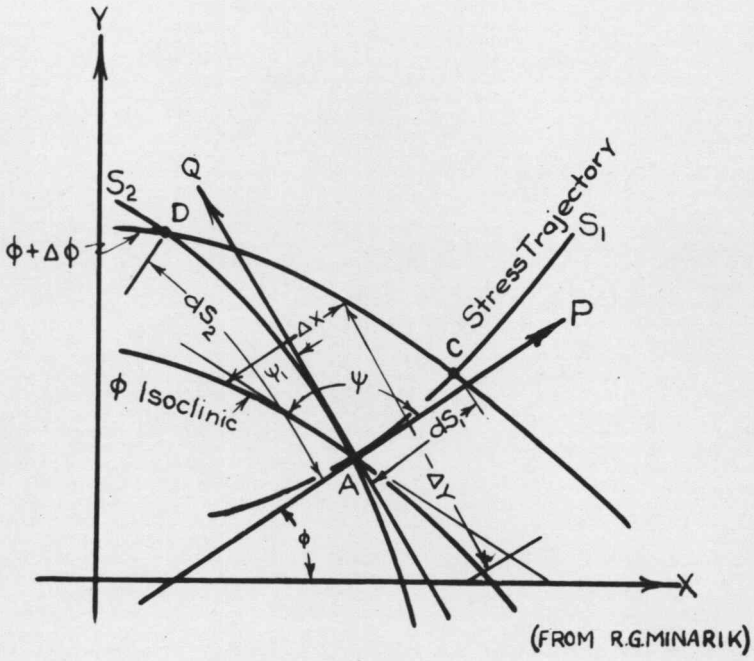

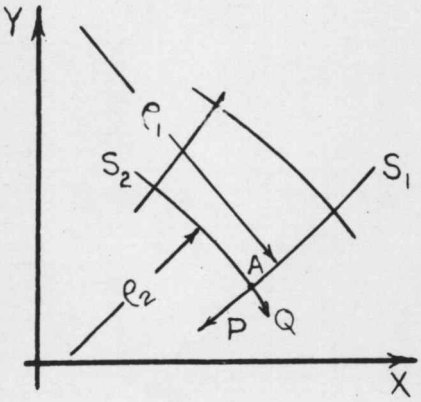

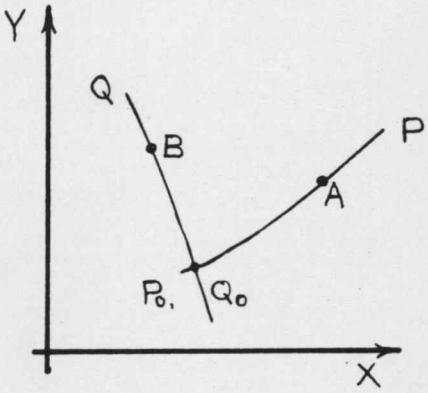

Fig.5.-Symbols Used in the Graphical Integration Method.

resolves itself into the evaluation of these two integrals which are definite functions of S and (P-Q). The quantity (P-Q) is fairly easy to determine from the order of the isochromatic, but ρ and ds are often very complex functions of X and Y. In some cases it is possible to determine them accurately but they are capable of presenting tremendous analytical difficulty.

The general method for the evaluation of equations 6 and 7 is as follows:

Referring to the upper diagram of Fig.5, it can be seen that

$$\frac{1}{\rho_2} = \frac{d\phi}{ds_2} \qquad 8$$

Also, through the point A passes the isoclinic of parameter ϕ. The line intersecting s_1 and s_2 at C and D is a near isoclinic of parameter $\phi + \Delta\phi$. Equation 8 then becomes

$$\frac{1}{\rho_2} = \frac{d\phi}{AD} \qquad 9$$

and since

$$ds_1 = AC \qquad 10$$

we have

$$\frac{1}{\rho_2} ds_1 = d\phi \frac{AC}{AD} \qquad 11$$

letting

$$\frac{AD}{AC} = - \tan \psi \qquad 12$$

where ψ = the counter-clockwise angle between the P stress trajectory and the isoclinic.

The equation 6 reduces to

$$P_A = P_0 - \int_{\phi_0}^{\phi} (P-Q) \cot \psi \, d\phi \qquad 13$$

any by symmetry-equation 7 can be written

$$Q_B = Q_0 - \int_{\phi_0}^{\phi} (P-Q) \cot \psi' \, d\phi \qquad 14$$

In the last expression ψ' is the counter-clockwise angle between the Q stress trajectory and the isoclinic.

Equations 13 and 14 are in a form which facilitates numerical computations since the indicated integrations can quite easilly be obtained graphically. It is only necessary to plot (P-Q) cot ψ against ϕ and determine the area under the curve with an ordinary planimeter. Values for P and Q for any point in the stressed model can be obtained provided P_0 and Q_0 are known. It is important to note that the integration must always proceed along the paths of the orthogonal stress trajectories.

Where the angle ψ becomes small or large, the cot. changes rapidly and any error in the angle measurement causes a large error in the final value of the stress. Resort is then made to the geometry of the figure and cot ψ determined in terms of the intercept in the P and Q directions between the isoclinic through the point and the neighboring isoclinic and the distance along the trajectory from the last isoclinic. Equations 13 and 14 then become:

$$P_A = P_0 - \Delta\phi \int_0^A \frac{(P-Q)}{dy} \, ds_1 \qquad 15$$

$$Q_B = Q_0 - \Delta\phi \int_0^B \frac{(P-Q)}{dx} \, ds_2 \qquad 16$$

where the only change is ds_1 and ds_2 which are the dis-

tances along the trajectory in question and y and x are intercepts made by the isoclinics.

(B) Graphical Method Developed by Dr. J. H. A. Brahtz (4).(6).

This method is essentially structural and was developed by considering the model composed of two systems of orthogonal arches given by the lines of principal stress. No shear but only normal forces exist along any element or block bounded by four principal stress lines, two from each system. The problem is then reduced to determining the force polygon, having given the funicular polygon and certain reactions. For the block or element being in equilibrium, the unit forces along each side may be considered as a concentrated total force normal to that side. The directions of the four forces being known, if the magnitudes of two of them are known or can be determined, the magnitudes of the other two may be found. In some cases the boundary stresses are known along two adjacent sides and a start may be obtained. From there on, each row of elements may be considered as a new boundary and the forces on the next row determined. This method has the advantage that it is fast, and everything is in plain view with many opportunities for continual check and adjustment.

C. Other Methods. A graphical method of constructing lines having a constant value for the sum of the

principal stress (P+Q) called "Isopachic lines" is described by Dr. H. P. Neuber.(15). From the two networks, (P+Q) and (P-Q), the individual stresses at any point can be determined but the method is quite involved. Prof. Coker (5) has used a method whereby measuring the change in thickness of the model under load, and with a knowledge of Poisson's ratio and Young's modulus, the value of (P+Q) can be determined at any point. The disadvantage of this method is that the deformations to be measured are in the order of millionths of an inch and reliable results are quite improbable.

Purely optical determinations are being developed at the present time for photographing fringes that show lines of constant (P+Q). (9). Another method used by Favre in Zurich consists of measuring, by the use of an interferometer, the retardation of a ray of plane polarized light when the plane of polarization coincides with the principal stress direction. This retardation is proportional to the stress.

A membrane analogy has also been developed in which the equation of the small ordinates of a membrane stressed with a constant tension and having the same pressure on both sides, is the same as the equation defining the distribution of (P+Q). A membrane may be stretched over a form whose height from a datum plane

is equal to the sum of the principal stresses at the boundary of a loaded model. The value of these stresses may be obtained from photo-elasticity. The ordinate from the membrane will then give the value of (P+Q) at any point.

Fortunately, the quantitative analysis is not the strongest point of photo-elasticity. The determination of the direction of stress at any point is, alone, of great importance. Also, the value of the maximum shear and the principal stress at unloaded boundaries is likewise of value. In many cases the maximum fiber stress is at a boundary, or the maximum shear may be the controlling factor for the material. Of no less importance is the fact that stress concentrations can be located from a glance at the loaded model. It can be said, therefore, that with the development of the technique of making and loading models and with some experience in testing, a large amount of pertinent information can be obtained in a reasonably short time.

PART III

PROCEDURE

PART III

PROCEDURE

1. General. If the optical apparatus is at hand and a material available that is free from initial stress, the following procedure can be followed. The model is laid out and machined with sharp tools, taking special precaution at all times not to apply undue forces to the material in any way that might set up initial stresses in the material that would otherwise not be present. A calibration member should be cut from the same material as the model, and if initial stresses are found in either, both should undergo the same annealing treatment. Assuming a suitable loading frame at hand, the known loads are now applied accurately.

From the observations, the isochromatics, or fringes should be sketched or photographed, and their fringe order determined from the calibration member. By simultaneously revolving the crossed Nicols, a complete network of isoclinics can be obtained and recorded. From these results the maximum shear can be determined at all points in the stressed model by noting the fringe order. A complete network of stress trajectories can be developed from the isoclinics, and then, by some method of analysis as previously explained, the magnitudes of the principal stresses, P and Q, aan be found.

2. Material Used. At the beginning of the investigation it was realized that trouble would be experienced with bakelite from induced initial stresses resulting from the drilling of the small rivet holes. With this in mind attempts were made to use the new material "Marblette", a synthetic resin which can be machined quite easily and still be comparatively free from initial stress. However, after conducting some modulus of elasticity tests on Marblette, it was found that at values of stress as low as 25 lb. per square inch the material was very plastic. As a result, the water white bakelite, BT-61-893, manufactured by the Bakelite Corporation especially for photo-elastic work was used. Its modulus of elasticity was also determined, using a pair of Huggenberger Tensometers, and found to be 650,000 pounds per square inch. The method of determining the modulus of elasticity is shown in Fig. 6.

3. Optical Apparatus Used. The photo-elastic apparatus in the Department of Mechanical Engineering at Oregon State College is shown in Fig.7 and in diagramatic form in Fig.8. The polarizer and analyzer are 15 mm. Ahrens, (Zeiss) prisms, making the size of the field obtainable limited only be the size of the lenses. The quarter-wave plates (Zeiss) were of mica and fastened to each prism case by a pivot so they could be swung out of the way when using plane polarized light. The

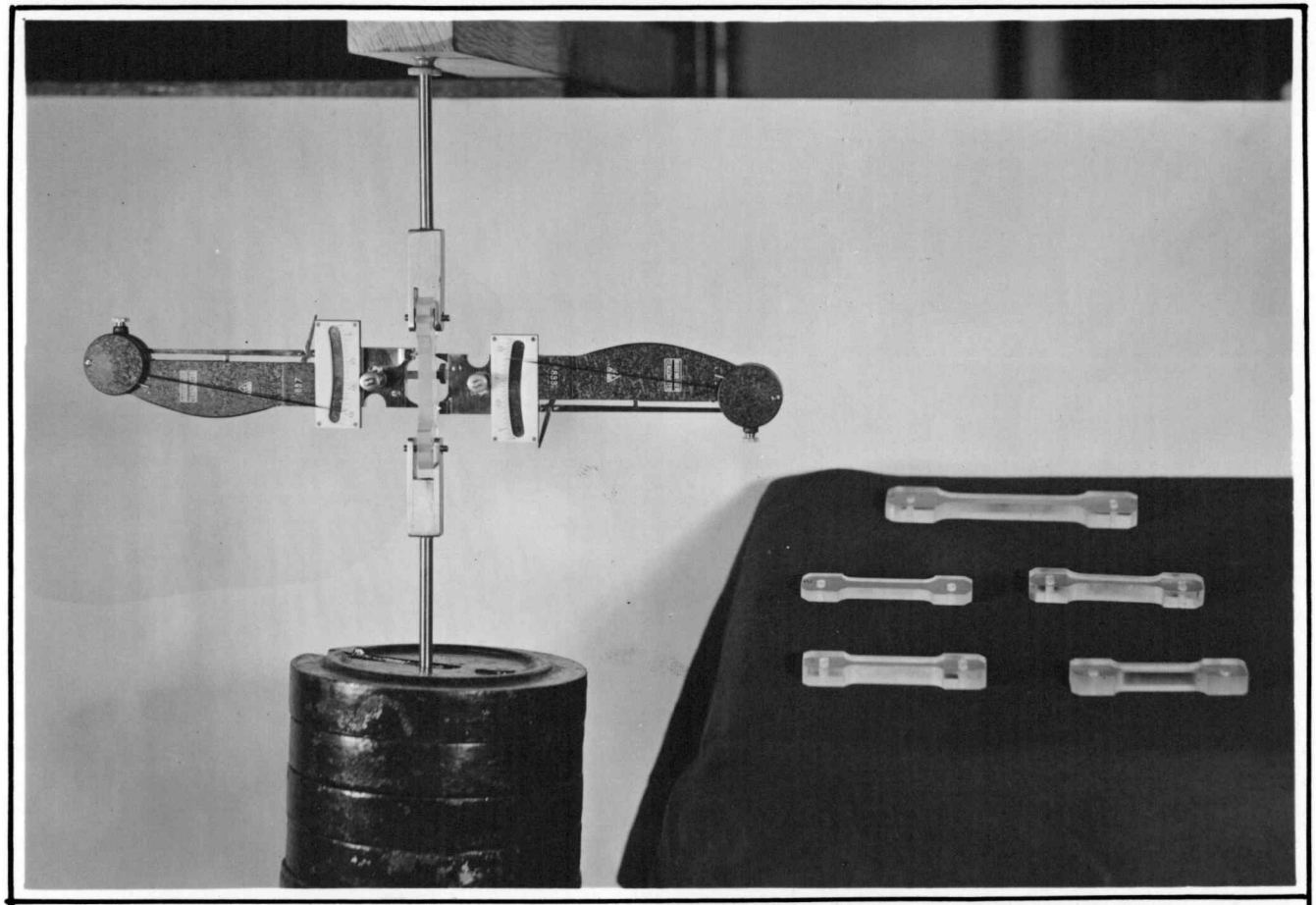

Fig.6.-Method of Determining Modulus of Elasticity Using Huggenberger Tensometers

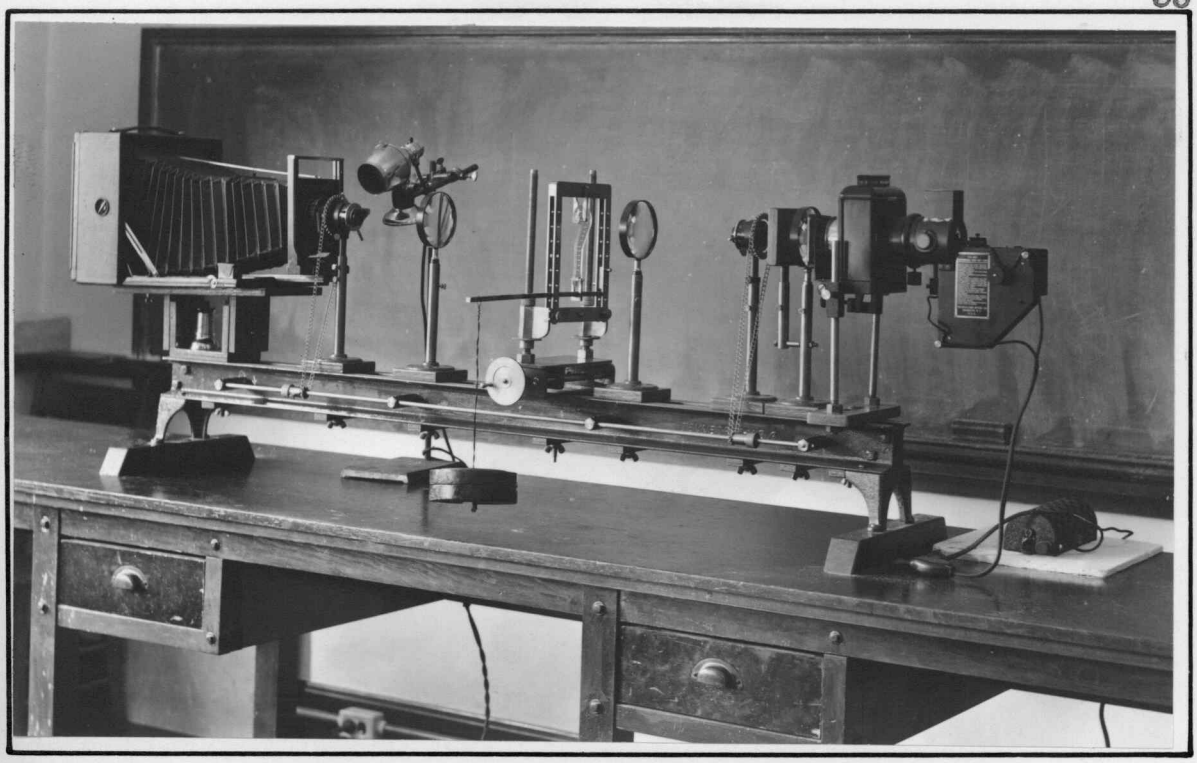

Fig.7.-Photo-elastic Apparatus.

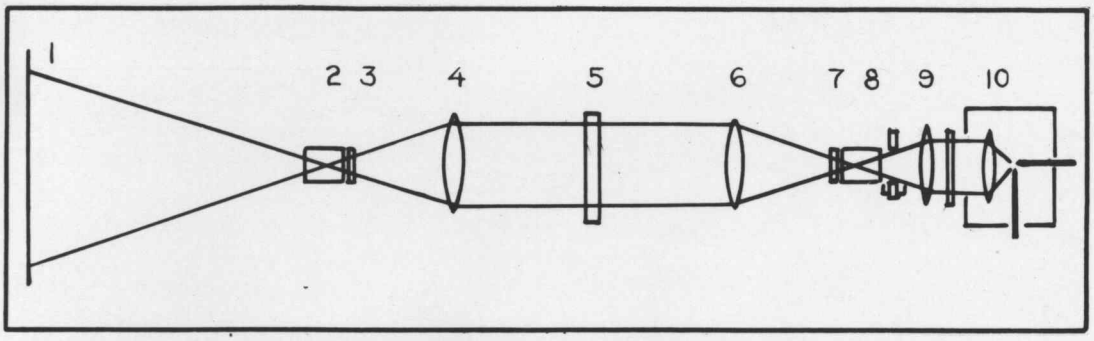

Fig.8.-Diagram of Apparatus.

1. Vertical drawing board or camera plate
2. Ahrens analyzing prism
3. Quarter-wave plate
4. Converging lens
5. Loaded model
6. Lens at focal length to obtain parallel beam
7. Quarter-wave plate
8. Ahrens polarizing prism
9. Converging lens followed by color filter holder
10. Carbon-arc source with lens and heat filter

axes of the mica plates were always kept at an angle of 45 degrees with the axes of the Ahrens prisms. One desirable feature of the apparatus is that the polarizer and analyzer can be simultaneously revolved by turning a single shaft. This is made possible through a system of chain gears connecting the shaft to the prisms and is certainly a great convenience when determining isoclinics.

4. Method of Recording Data. As soon as the model was in position and the load applied, a photograph was taken with the quarter-wave plates in place. For taking photographs, Wratten filters, Nos.G-15 and H-45, were used, as these gave a very narrow band of light that closely approached a monochromatic beam. Also, with this combination of filters the deepest fringe patterns and the sharpest lines resulted when photographed.

Removing the quarter wave plates, the isoclinics were sketched for different orientations of the crossed prisms. For sketching purposes the camera was removed and a vertical drafting board substituted in its place. It was found that greater accuracy could be obtained in determining the isoclinics by merely projecting the image on a sheet of sensitized photographic paper. The sensitized sheet was placed in a printing frame and held in place against the vertical drafting board where it was exposed for a period of fifteen seconds. The

resulting print was just opposite in black and white fringes than actually viewed, but was of great help in accurately determining the isoclinic lines. A print was made in this manner along with the sketch for each angular setting of the crossed prisms.

In connection with obtaining the isoclinics, it was found that in some sections of the model, using bakelite, the weaker isoclinics seemed to merge into the more pronounced isochromatics, making it difficult to obtain them accurately. It was also found that with a Marblette model and with a very small applied load only a few isochromatics were present but the isoclinics were readily discernable in all portions, (See Fig.18), and were identical, in position, with the same isoclinics that were apparent in the bakelite model. Marblette models consequently were substituted for bakelite models in this connection.

5. Preparation of Models. The size of the models was limited by the available diameter of the beam of light, this being approximately 3 inches. As the length of the prototype hooks was close to twelve feet, a model to scale of one inch equals fifty inches would just fit into the light beam. For a plain hook model, no trouble was encountered, but the drilling of the small rivet holes in the hooks as designed proved to be very difficult using such a reduced scale. As

a result, it was decided to use a larger scale, one inch equals twenty-five inches, and to study the hook in two sections as either the top or the bottom would just fit into the light ray. Even with a ratio of one inch equals twenty-five, great care had to be taken in drilling the small holes, as the initial stresses caused by drilling could otherwise not be completely removed by annealing.

The procedure in making the models was as follows: The dimensions of the model were carefully laid out on rough bakelite and the outline of the finished model carefully scribed. Then, using a small power driven jig saw, the blank models were cut from the bakelite stock, taking care not to rush the sawing process and to leave a little material for finishing the edges. The finishing process was accomplished by filing to exact dimensions, using light strokes of the file and making sure that the file was at all times clean and sharp. Drilling operations were performed on a small precision high speed drill, and very little pressure was applied to the drill. The polishing process was carried out by first sanding the surface by hand, using fine sandpaper (000)-and then finishing on metallographic polishing laps in the same manner as metal specimens are prepared for examination. After this, the specimens were annealed, if necessary,

and then placed in the loading frame. It should be mentioned here that bakelite trunnions were also made to scale so as to assimilate the same conditions of contact as would be present in prototype loading.

For the annealing process, the usual methods of annealing bakelite were all tried, but it was found that the initial stresses around the small holes could not be completely removed. After much experimenting, it was learned that by placing the models in an oil bath, higher temperatures could be used without fogging or changing the properties of the material in any way. The final method of annealing used was as follows:

The models were placed in a bath of ordinary lubricating oil and gradually heated to a temperature of from 240-250°F. After a three-hour soak at this temperature the source of heat was removed and the whole container allowed to cool to room temperature. An ordinary two gallon pail was used for this process, the heat being supplied by a small gas burner. Calibration and tension members were subjected to the same treatment and it was found that the physical and optical properties of the bakelite were in no way altered.

6. Loading Frame and Method of Loading. To accomodate the enlarged hook model (scale 1"=25"), a loading frame was constructed, the design of which was such that the model could be moved horizontally or vertically

in the light beam without changing the load. Other necessary construction was included in the design of the frame so that it could be universally used to accomodate tension or bending models.

All loads were applied through levers acting on knife adges, great care being taken at all times to accurately maintain correct lever arm ratios. Fig.10 shows the loading frame and the method of applying the load.

7. Calibration of Fringe Orders. The method of determining the magnitude of the fringe orders was by the use of a calibration beam loaded at points equidistant from the ends so that the portion of the beam in constant bending sustains no shear. Fig. 11 shows three beams loaded in such a manner that the bending moment in all three is the same. As a matter of interest, one beam of 3/8" bakelite and two beams of 1/4" bakelite were loaded at the same time for purposes of comparison and checking. For all models, 1/4" bakelite was used.

Tables I and II give the data used in determining the magnitudes of the fringe orders in the different beams. It will be noted that the extreme fiber stress was not used since, from the photograph of the fringes, considerable edge stress is indicated by the unsymetrical number of fringes on opposite sides of the neutral axis. In each case the neutral axis was in the center of the

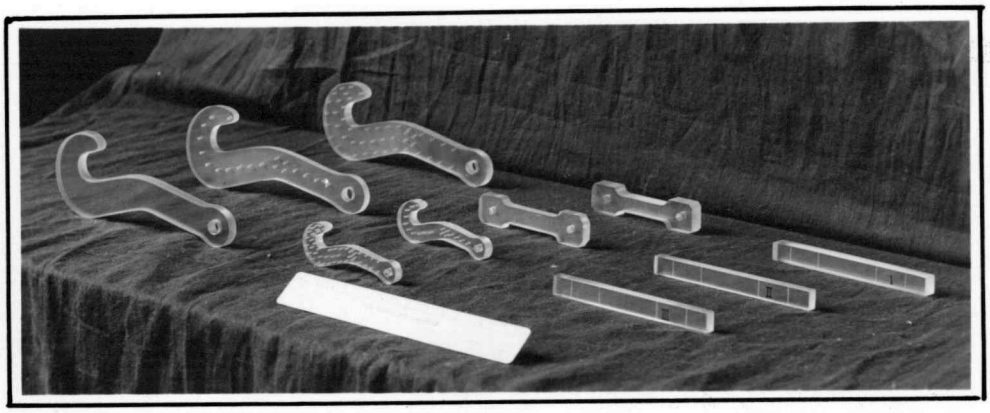

Fig.9.-Hook Models, Calibration Beams and Tension Members

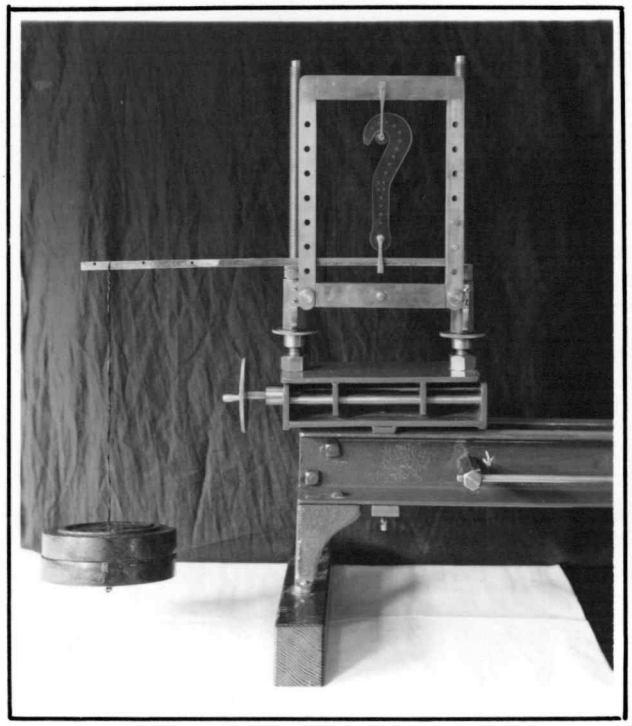

Fig.10.-Loading Frame with Model in Place

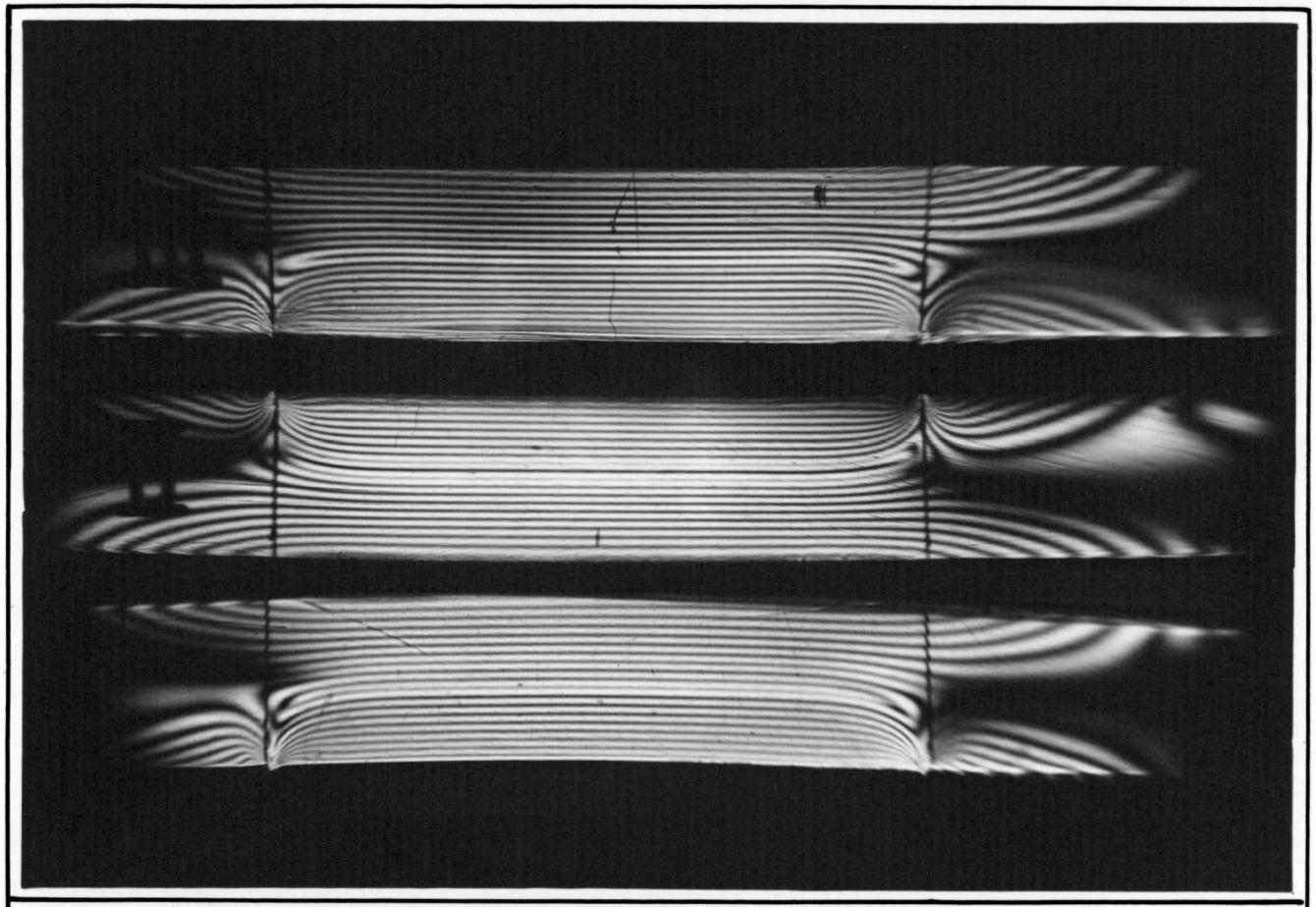

Fig.11.-Fringe Photograph Showing Three Calibration Beams Under Equal Bending Moments

beam. Points on each side and equidistant from the neutral axis were chosen where fringes were still symetrical. The fiber stress was calculated by the formula S= My/I and divided by the number of fringes between the point and the center. This value was then taken as the magnitude of the fringe order. That is, if the fringe order was 315 lb. per sq. inch, a fringe of the fourth order would represent a stress at 4x315 or 1260 lb. per sq. inch.

8. Steel Models Tested. As a method of checking the photo-elastic analysis, three steel models were made to the exact dimensions of the corresponding bakelite models, (scale 1"=25"). Two tensile bars were cut from the same material as the steel hooks for the purpose of determining the yield point of the material. Knowing the stress in the section of maximum moment as determined from the photo-elastic results for a given load and the yield point of the material from which the steel models were made, it was possible to calculate the load on the steel models that would cause yielding. The steel models were whitewashed and placed in a loading jig that was gripped in the jaws of a 30,000 lb. Olsen universal testing machine. The yield point of the models was observed both by the flaking of the whitewash in the section of maximum moment and also by the use of a Last Word gage, sensitive to

TABLE I

CALIBRATION BEAM DIMENSIONS

Beam No.	Length	Thickness	Depth	Section Modulus $\frac{I}{C}$	Young's Modulus
	inches	inches	inches	in.^{3}	#/sq. in.
I	3.00	0.389	0.408	0.0108	710,000
II	3.00	0.263	0.404	0.0071	650,000
III	3.00	0.263	0.413	0.0074	650,000

TABLE II

DETERMINATION OF FRINGE MAGNITUDE

Beam No.	Moment	Max. Fiber Stress	Dist. from Center to point Calculated	Fiber Stress at Calculated Point	No. Fringes at Calculated Point	Fringe Magnitude
	in.lb.	#/sq.in	inches	#/sq.in.		#/sq. in.
I	22.50	2075	0.179	1820	8	228
II	22.50	3140	0.162	2520	8	315
III	22.50	3180	0.191	2810	9	313

0.0001 inches. The strain gage was so attached to the model that it measured any opening that might occur in the mouth of the hook, thus making it possible to observe any yield in the model and the corresponding load to produce the same. Fig.12 illustrates the method employed in testing the steel models.

After the load producing the yield point was found, the models were photographed (Fig.13) showing the flaking off of the whitewash in the section of maximum stress. The tests were then continued to what might be termed destruction, the load being observed for corresponding deformations in the three models.

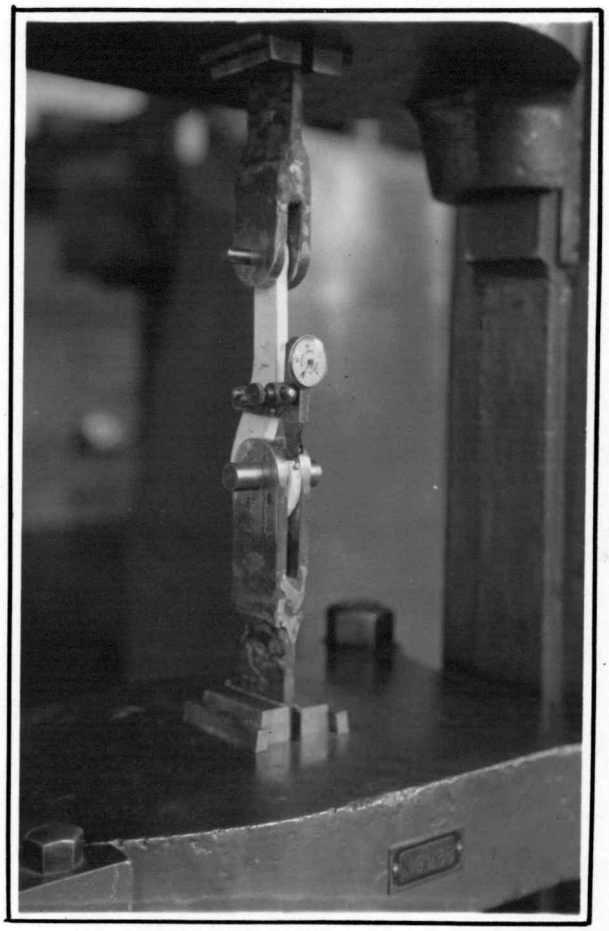

Fig.12.-Steel Hook Model in Place for Testing

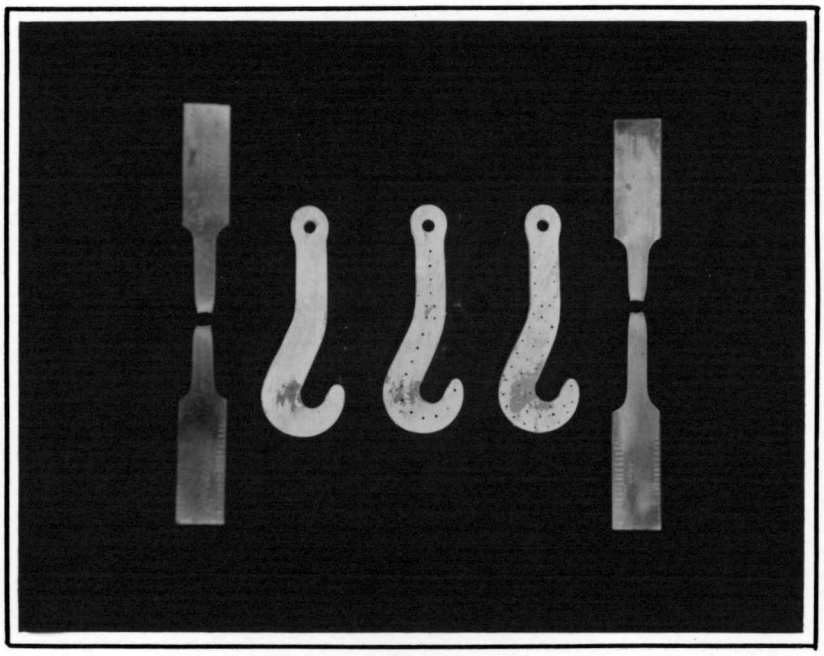

Fig.13.-Steel Models and Yield Bars.Note Flaking of Whitewash in Section of Maximum Stress

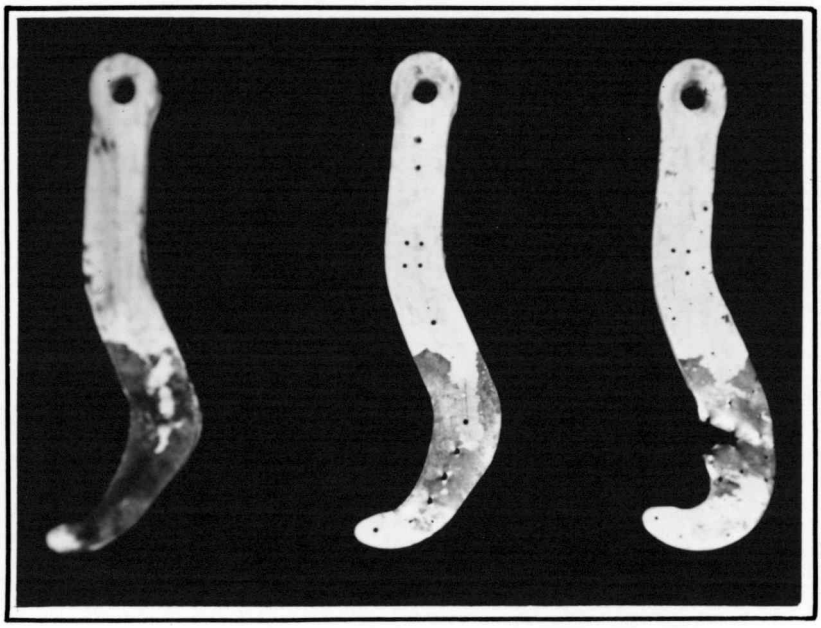

Fig.14.-Steel Models after Failure

PART IV

INTERPRETATION OF RESULTS

PART IV

INTERPRETATION OF RESULTS

1. Reference to Prototypes. Before discussing the results of the investigation, something should be said concerning the design of the prototype hooks. As mentioned previously, the hooks studied were two sixty-two and one-half ton ladle hooks, the design having been submitted by the Morgan Engineering Company. These large hooks are used in the steel industry in pairs, one on each side of the ladle as shown in the Frontispiece. Being manufactured in a laminated design, the eight 5/8 inch plates are fastened together by the use of rivets and the two designs, as shown in Fig.15, are different only in the location of the rivet holes. In this study, no attempt was made to analyze the hooks as they are actually manufactured, i.e. laminated plates riveted together. Such a model would not lend itself to a photo-elastic investigation for various reasons. Consequently, the hooks were studied as a solid mass having a homogeneous rectangular cross section, the models being made of one piece of material. This factor should have no effect whatsoever on the correlation of results between the models and the prototypes.

Along with the tests on the models of the proto-

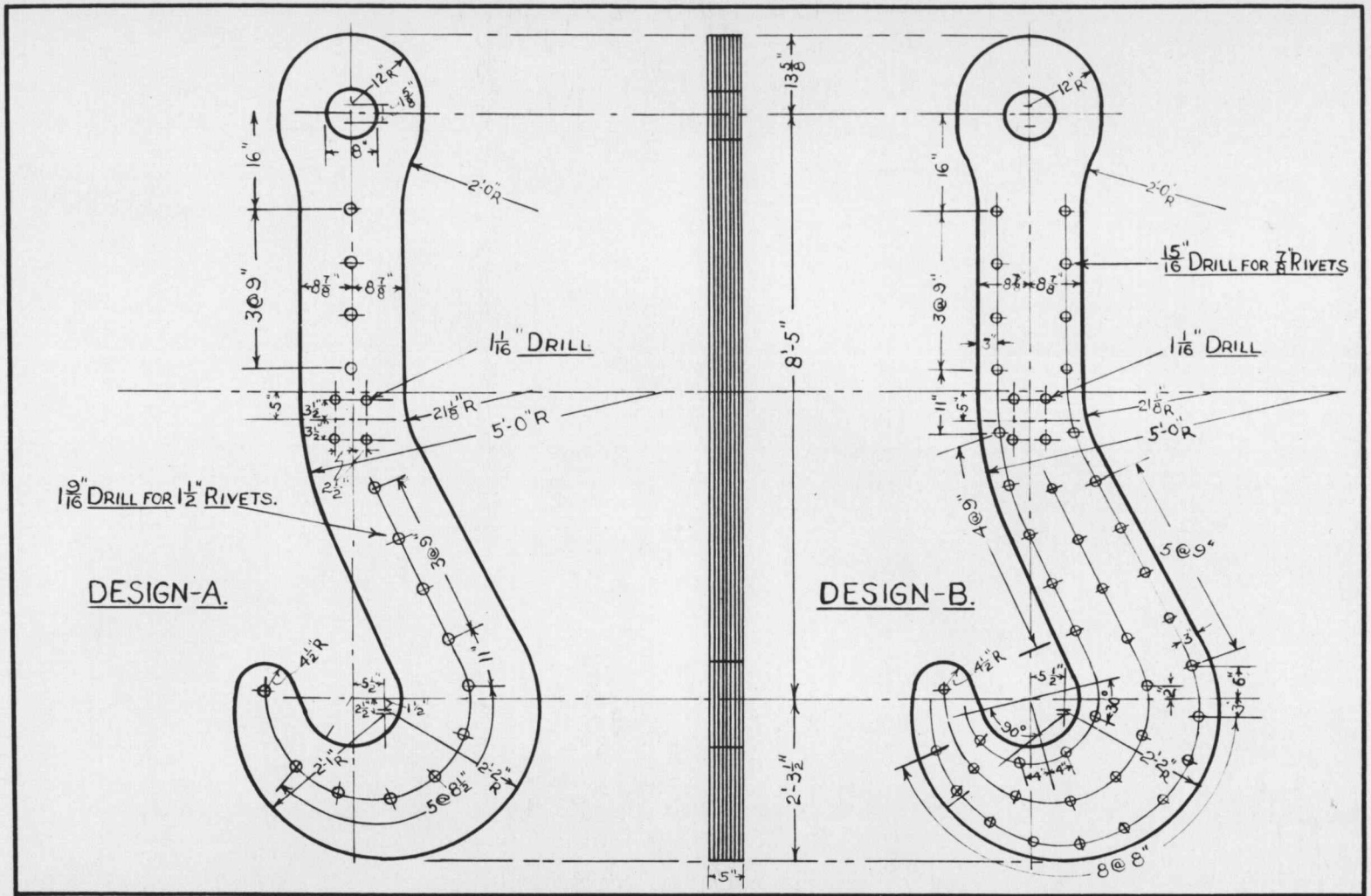

Fig.15.-The Two Morgan 62.5 Ton Ladle Hook Designs.

types a third model of a plain hook was studied. This model had no rivet holes, and from the analysis of it reference could be made concerning increased stresses at any points in the prototype models that resulted from the influence of the rivet holes. Throughout this discussion the models will be referred to as follows: The design having the rivet holes located in the geometric center will be designated as "Design A"; the design having the rivet holes distributed in three concentric rivet lines as "Design B"; and the reference model having no rivet holes as "Design C".

2. Boundary Stresses in Three Designs Studied: Fig.16 shows the fringes or isochromatics resulting from a load of thirty pounds on each of the models investigated. These fringe photographs were obtained from models having a scale ratio to the prototype of one to fifty and can only be used as comparative views of the general distribution of the stresses in the respective designs. In designs A and B, the rivet holes are slightly larger than the scaler dimensions and in design C, the initial stresses could not be completely removed. Consequently, models constructed to this scale were not used for any of the analyses. Because of optical reasons, rivet holes appear somewhat larger, in proportion, than were the holes in the

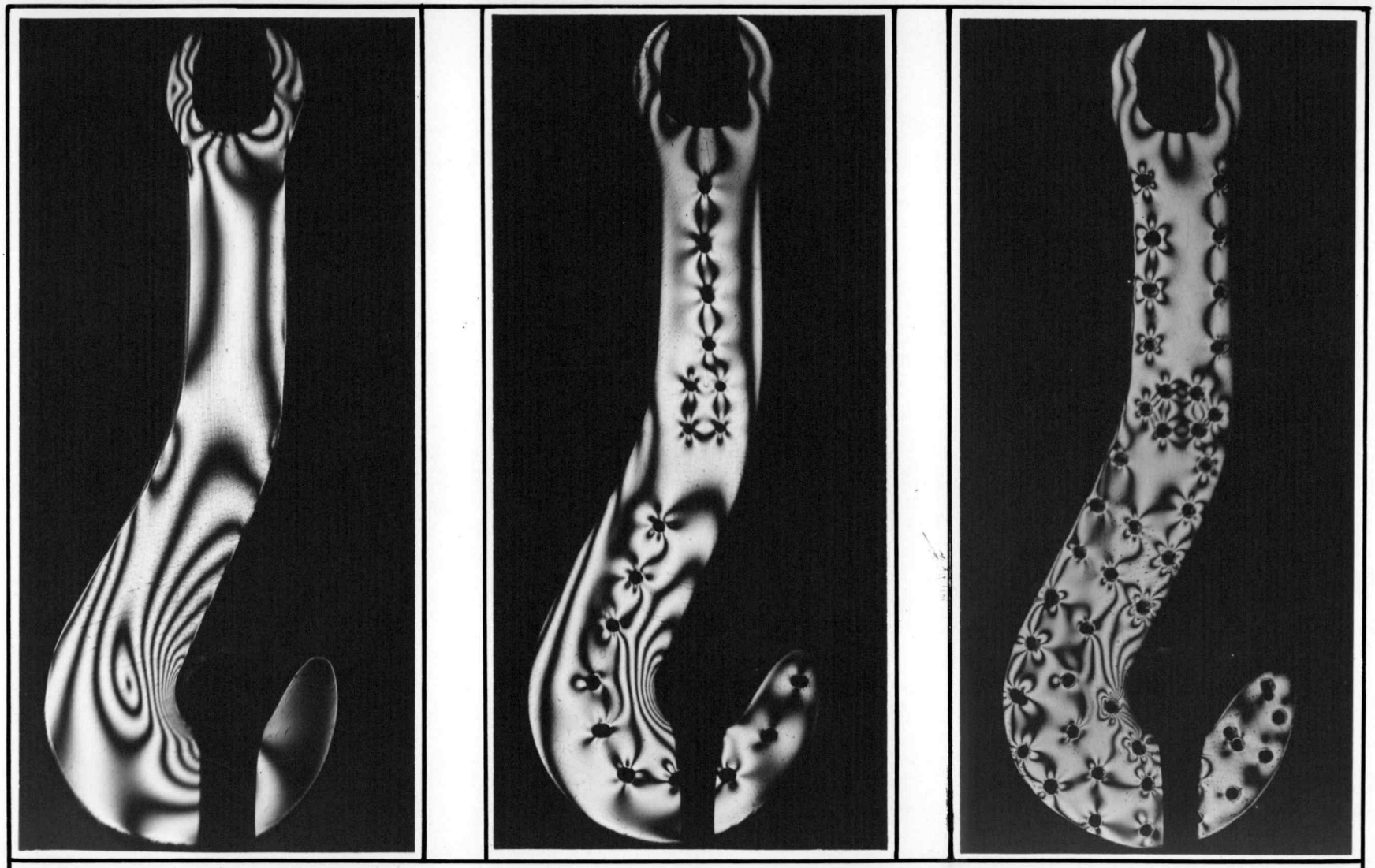

Fig.16.-Isochromatic Lines for Three Model Designs.Scale of Models-1"=50".

models.

Figs. 17, 19, and 20 show the corresponding fringes in models of a scale ratio to the prototype of one to twenty-five. In each case, the load on the bakelite model was eighty pounds. Nine fringes, corresponding to a fiber stress in the model of 2835 lb. per sq. in., are discernable in both design A and design C, whereas, eleven fringes, corresponding to a unit stress of 3,465 lb. per sq. inch, are discernable in design B. From this evaluation it becomes apparent that the rivet holes, when located in the geometric center, have little or no effect on the critical stress. However, in comparing results of design C with the reference model, it is noticed that the effect of the rivet holes is to produce a stress increase factor in the critical section of 1.22 times the stresses in the plain hook.

In Fig.19 it is readilly noticed that stress concentrations around the holes have very little influence on the critical stress in the section of maximum moment. In Fig.20, however, the locations of the rivet holes are such that not only is stress concentration around the holes increased but also the critical stress in the section of maximum moment as well. Remembering, now, that at an unloaded boundary, one of the principal stresses is equal to zero, the isochromatics are a direct measure of the other principal stress and it is

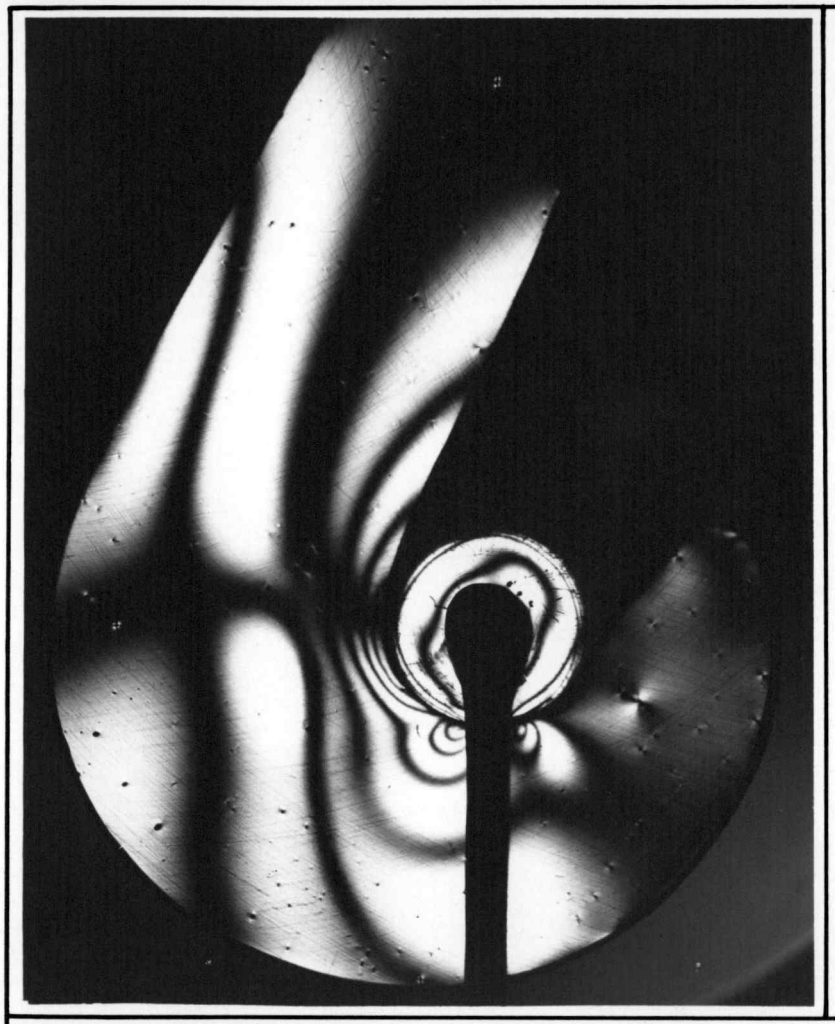

Fig.18.-Isoclinic Lines in Marblette Model

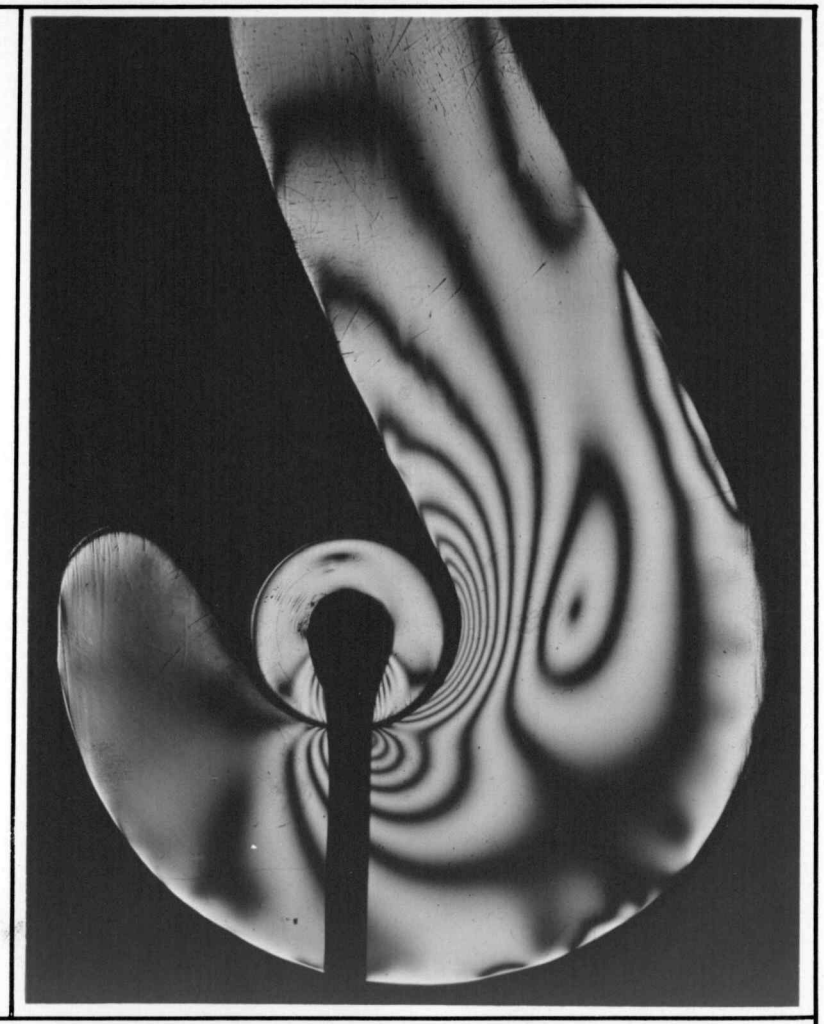

Fig.17.-Isochromatics in Reference Model
Load on Model = 80 lb. Scale-1"=25"

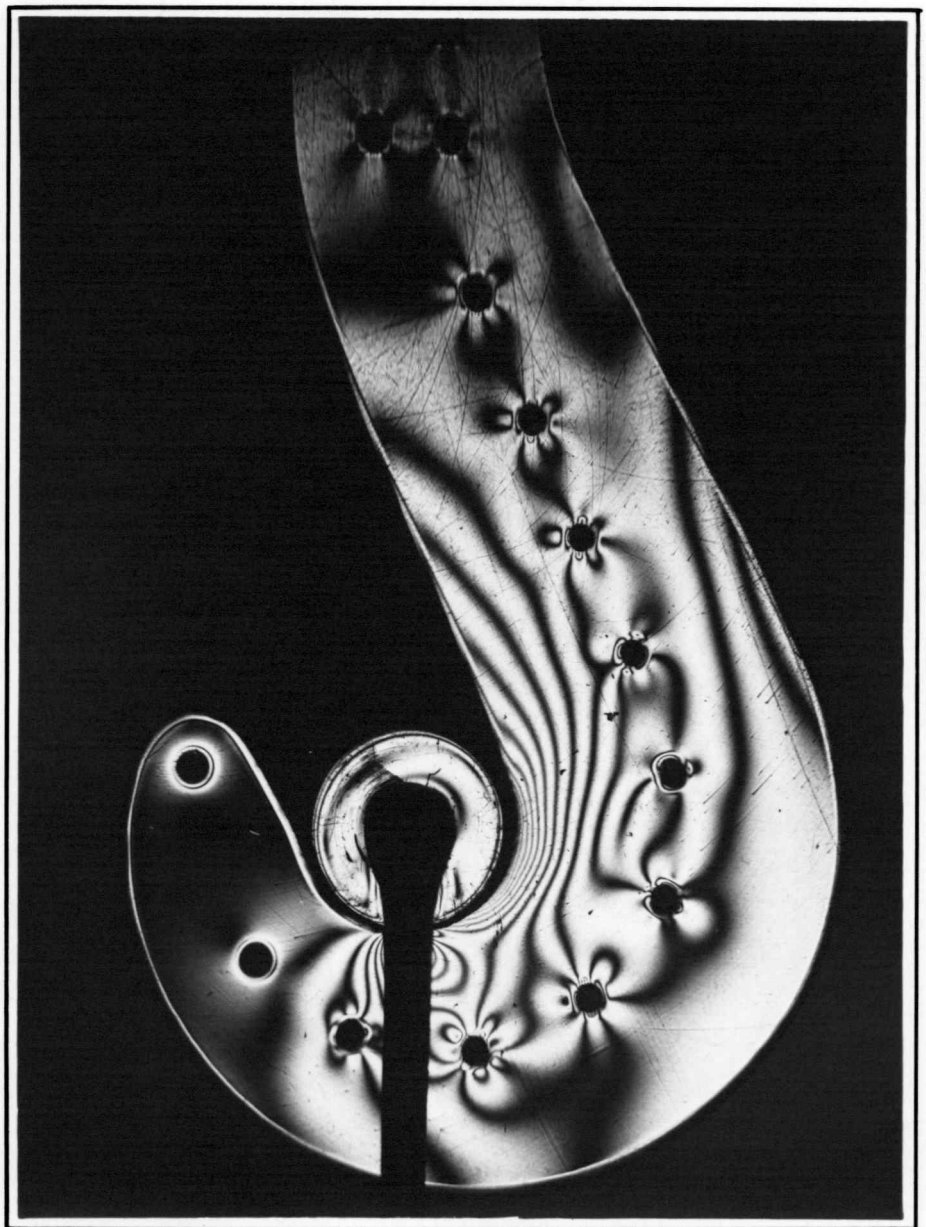

Fig.19.-Fringes in Design A. Load on Model = 80 lb.
Scale of Model-1"=25".

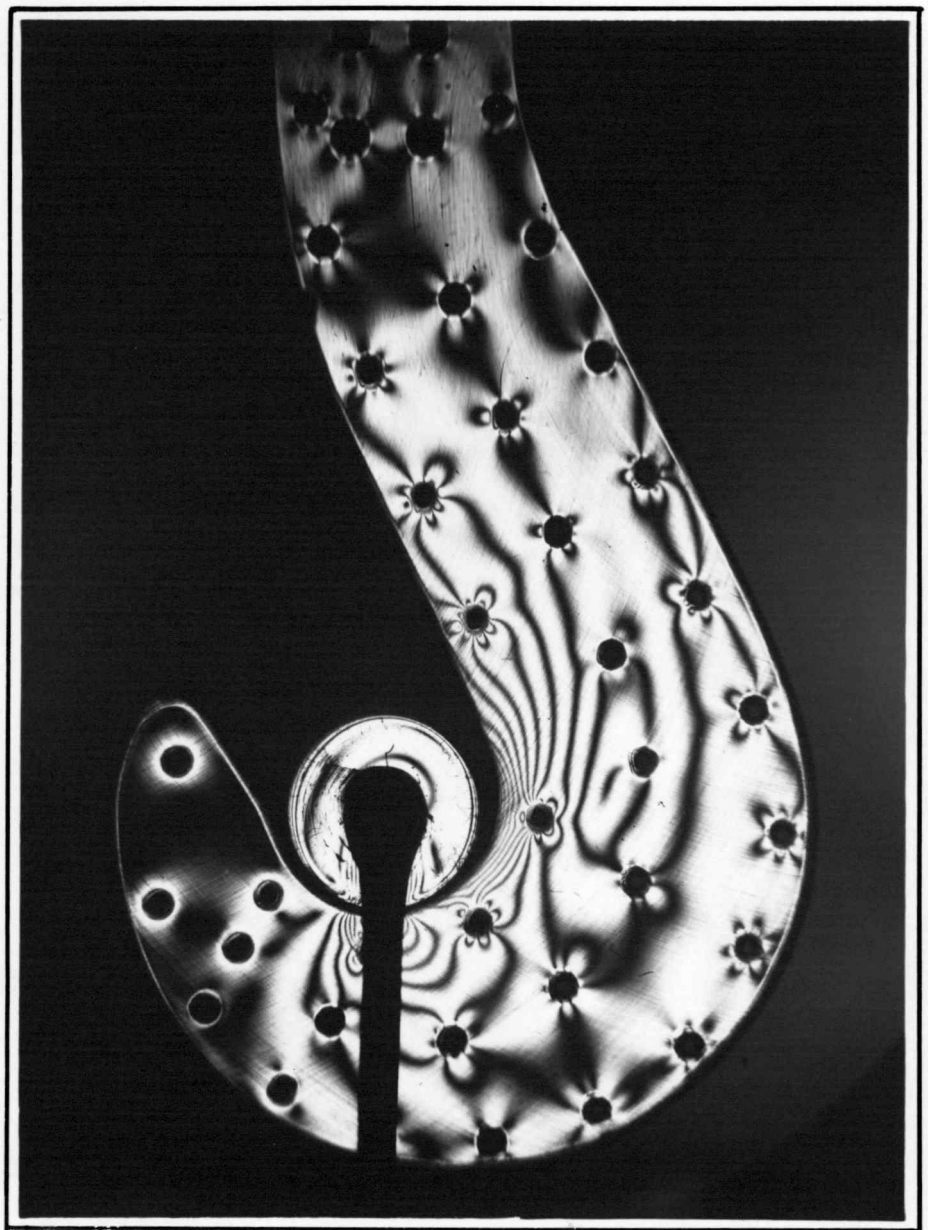

Fig.20.-Fringes in Design B. Load on Model = 80 lb.
Scale of Model-1"=25"

therefore possible to determine directly the magnitudes of the stress concentrations at the rivet holes. Referring to Fig.20 again, it can be seen that at the rivet holes the maximum order of the highest isochromatic is nowhere greater than the fourth and consequently, the value of the maximum stress at any of the rivet holes is less than half of the maximum stress at the critical section of maximum moment. For this reason, interest in this investigation was not directed to the magnitude of the stress concentrations at the rivet holes, but rather to the effect of the rivet holes on the maximum stress occurring at the critical section.

Much investigational work has been done in connection with stress concentrations due to rivet holes in different kinds of cross sections under various types of loading. (5-Chapt.6). From these investigations it may be said that no one solution can be applied to any two different types of conditions and many times not even to two similar conditions. Also, any results that might be obtained in connection with the stress distribution around any open rivet hole would not agree with results obtained were the rivet in place, and to obtain accurate results for the specific case the size of the model would have to be greatly increased and each rivet hole analyzed individually.

For these reasons, no attempt was made to analyze the stresses at the rivet holes but rather to investigate their effect on the ultimate performance of the prototypes as complete units.

3. Application of the Winkler-Bach Equation:

Because of the fact that it is comparatively simple and because it is applicable with a reasonable degree of accuracy for the solution of so many problems dealing with the curved beam under stress, the Winkler-Bach equation is commonly accepted. As previously discussed, this theory takes account of curvature and is based on the hypothesis that plane transverse sections remain plane after loading. This equation is derived in F.B.Seely's "Advanced Mechanics of Materials" (16:110), and will only be stated here in its familiar form. The equation is:

$$S = \frac{M}{aR}\left(1 + \frac{1}{Z}\,\frac{y}{R+y}\right)$$

where S is the unit stress at a distance y from the centroidal axis of the section

M is the bending moment at the given section

R is the distance of the centroidal axis of the section to the center of curvature of the unstressed beam

a is the area of the cross section

Z is a property of the area similar to the moment of inertia in the straight beam formula.

For a rectangular cross section, Z may be obtained from the following equation:

$$Z = -1 + \frac{R}{H} \left(\log_e \left(\frac{R+c}{R-c}\right)\right)$$

where $c = 2H$ and H is the width of the section with R as above.

Applying the Winkler-Bach equation to the plain bakelite model of scale 1" = 25", the results follow:

where $P = 80$ lbs. $R = 0.790$ in.

$a = 0.244$ sq.in. $y = -0.470$ in.

$M = 63.2$ in lb. $Z = 0.151$

giving $$S = \frac{80}{0.244} \frac{(-63.2)}{0.244 \times 0.790} \left(1 + \frac{1}{0.151} \frac{-0.470}{0.790 + (-0.745)}\right)$$

$$= 328 + (328)\ (1 + (-9.75)$$

and $S = 3188$ lb.per sq.in. at the outer fiber.

From the photo-elastic results the value was found to equal the fringe order at the critical section multiplied by the fringe magnitude or 9 x 315 lb.per sq.in., giving a unit stress of 2,835 lb.per sq.inch. Dividing this value into the value obtained by the Winkler-Bach equation gives a factor of safety of 1.12 in favor of the Winkler-Bach equation for the particular design.

4. <u>Correlation of Model Results to Prototype Analysis</u>. It has already been shown that from the photo-elastic analysis of the 1:25 scale models the stresses produced from a load of 80 pounds were 2835 lb.per sq.in. for designs A and C and 3,465 lb.per sq.in. for design B. As the thickness of the scale

models was 0.260 inches rather than 5.0/25 or 0.200 inches for the scale ratio, it is necessary to evaluate the model stresses for a corresponding load acting on the reduced area. Since the photo-elastic results take into account the composite result of all the stresses acting, this can be done by multiplying by the inverse ratio of the thickneses of the models. For a load of 80 pounds, the corresponding stresses become,

$$2{,}835 \text{ lb.per sq.in.} \times \frac{0.26}{0.20} = 3{,}690 \text{ lb.per sq.in.}$$

for designs A and C and 4,500 lb. per sq. inch for design B. Reducing these values to unit load conditions, a one pound load on the models would produce corresponding stresses of 46.12 lb. per sq.in. and 56.2 lb. per sq.in. respectively.

By conditions of similitude, the cross-sectional area of the prototype, having a linear dimension ratio of 25:1, would vary as the square of the linear ratio or as 625:1. Therefore, it can be said that for the plain hook, design C, a load of 625 lb. on the prototype would produce a corresponding unit stress of 46.12 lb. per sq.in. Since the design load of the prototype is 62.5 tons or 125,000 lbs. it is now possible to determine the maximum fiber stress for this load. Dividing the design load by the unit load, $\frac{125{,}000 \text{ lb.}}{625 \text{ lb.}}$ and multiplying by the unit stress,

46.12 lb.sq.in., a value of 9,224 lb.per sq.in is obtained which is the stress in the section of maximum moment resulting from the design load for the prototype models of designs A and C. Similarly, the stress in the prototype of design B for a load of 125,000 lb. is found to be 11,300 lb. per sq.in.

Applying the Winkler-Bach equation to a prototype model of a plain hook sustaining the design load, a stress value of 10,363 lb. per sq.in. is obtained. Dividing this value by the corresponding value obtained from photo-elastic calculations, a safety factor of 1.12 again results in favor of the Winkler-Bach equation. This would indicate that as long as the Z factor in the Winkler-Bach equation is the same, the unit stresses would vary directly as the cross sectional areas.

5. Determination of Circumferential and Radial Stresses. Fig.18 shows the isoclinic lines for the 45° setting of the crossed prisms with the reference axis, while Fig.21 is a reproduction of the sketched isoclinics for different settings of the crossed prisms. The reference axis makes an angle of 45° with the vertical plane of the hook so that a zero isoclinic is the locus of the points whose direction of stress is 45° from the vertical. The prisms are given a clockwise rotation and the angle measured from the

zero isoclinic. A 15° isoclinic, therefore, denotes all the points in the stressed model where the direction of stress is 15° clockwise from the zero isoclinic or 30° from the vertical. Proceeding in this manner, the short perpendicular lines were drawn over the isoclinics with Fig.22 as a result. Starting from any convenient point, as a point on a boundary, lines may be drawn in one of the directions of the short lines. This determines one system of stress directions. The other system is obtained by drawing the second set of lines normal to the first set, resulting in a complete set of stress trajectories as shown in Fig.23.

From an inspection of the resulting principal stress trajectories, it can be seen that at all points through the section of maximum moment, the circumferential (P) stress is at all points in a plane parallel to the vertical axis of the hook, and that the radial stress (Q) is at all points parallel to the horizontal axis of the hook. Since the plane of maximum shear is at an angle of 45° to the plane of the principal stresses, it becomes apparent that at all points on this line of maximum moment the maximum shearing stress occurs in a plane that is 45° with the vertical or horizontal geometrical axis. Referring to Fig. 17 again showing the isochromatics (P-Q) or lines of constant maximum shear it is possible to

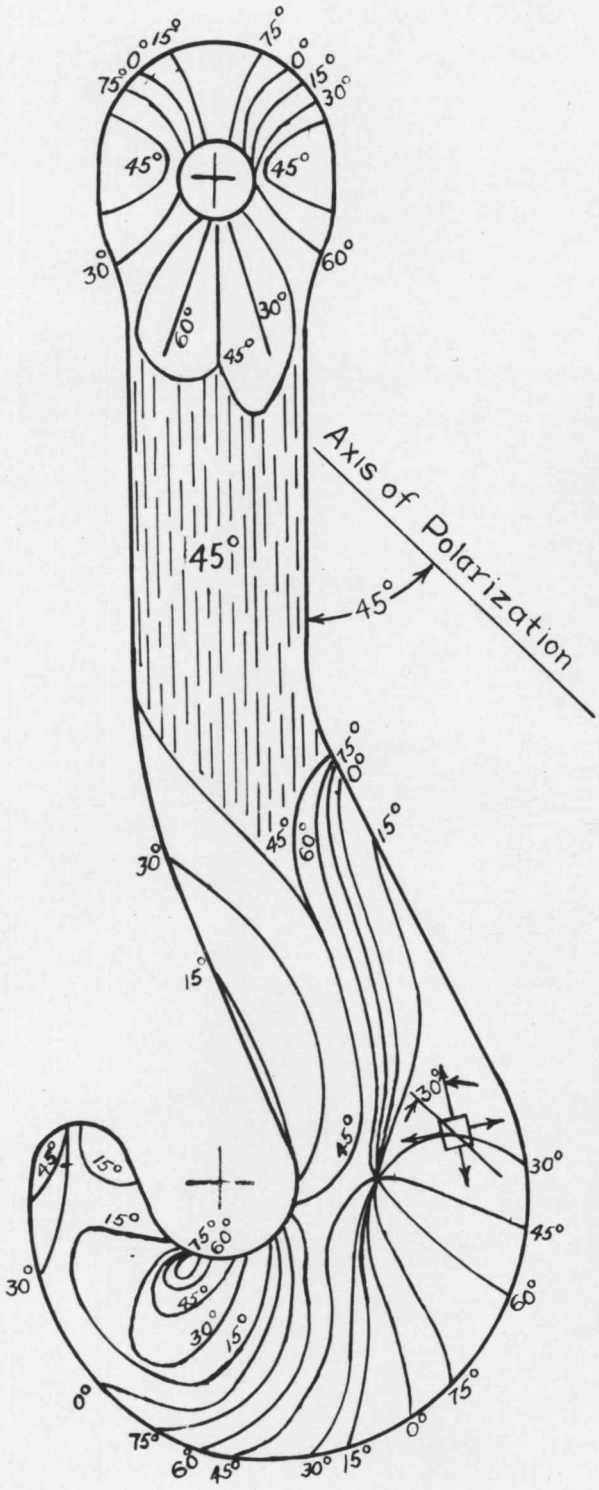

Fig.21.-Isoclinic Lines for Plain Hook Model. (Design C)

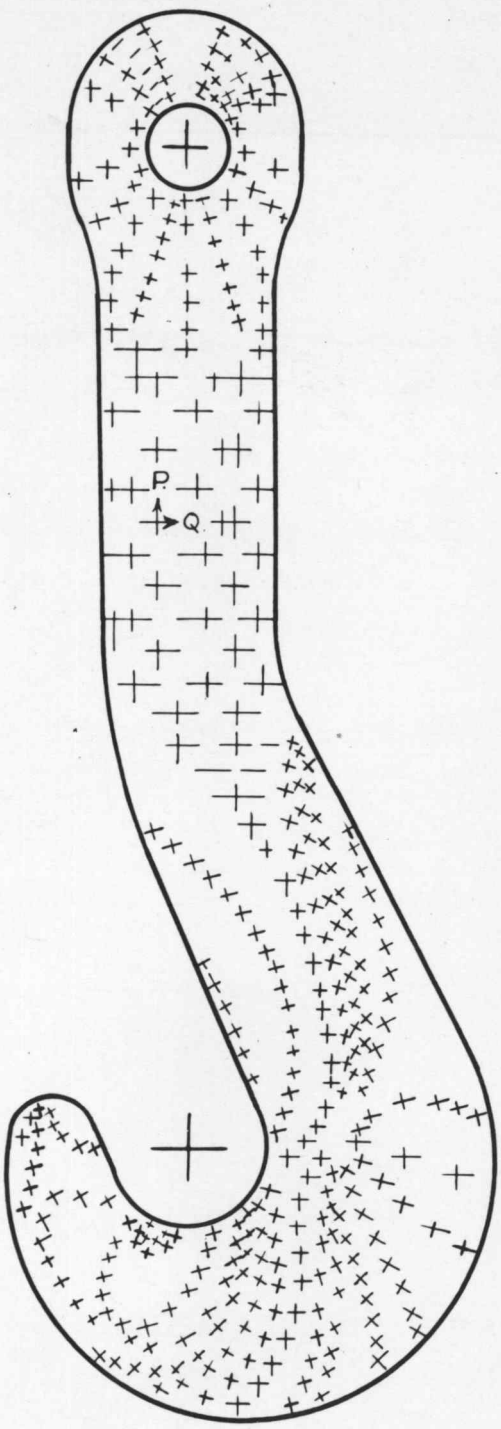

Fig.22.-Method of Determining Stress Trajectories from Isoclinics.

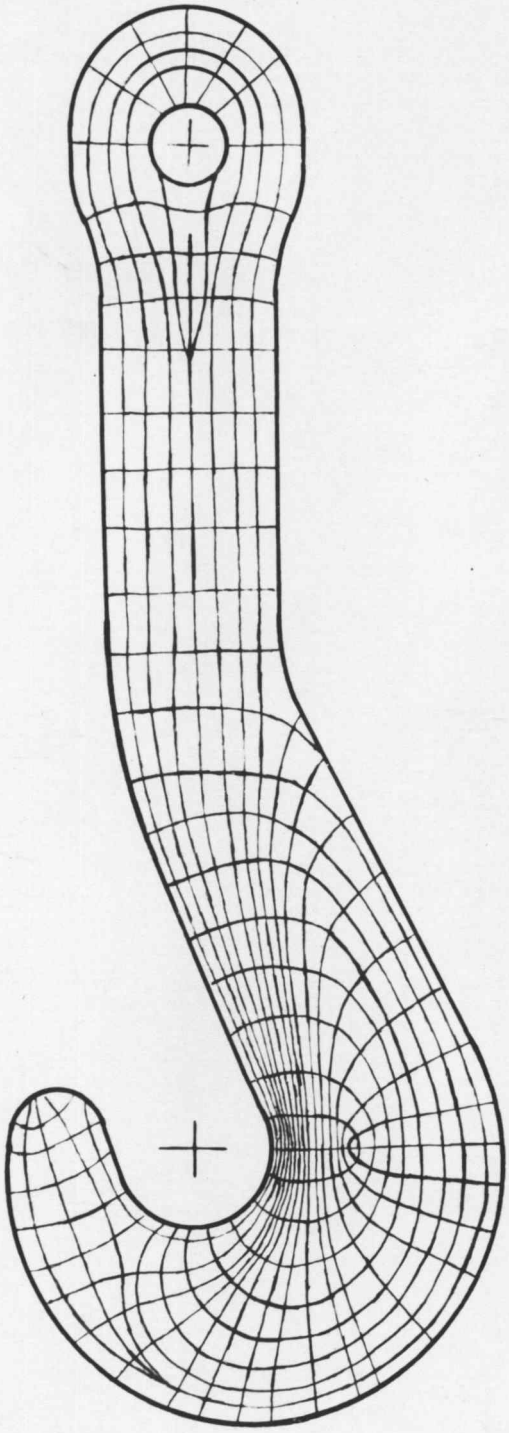

Fig.23.-Stress Trajectories for Plain Hook Model.

plot a curve of the maximum shearing stress for any point along the section of maximum moment as in Fig.24. From this information, both the intensity and the plane of maximum shear are known for any point along the horizontal section. It should be noted that Fig.24 is constructed in terms of the prototype hook sustaining the designed load of 125000 pounds.

From equations 13 and 14 as previously derived we have, in terms of x and y,

$$P_x = P_o - \int_{x_o}^{x} (P-Q) \cot \psi \, dx \qquad 13$$

and

$$Q_x = Q_o - \int_{x_o}^{x} (P-Q) \cot \psi' \, dx \qquad 14$$

where ψ is the counterclockwise angle between the P stress trajectory and the isoclinic. Since the P and Q stress trajectories are everywhere perpendicular and horizontal, and the plane of maximum shear is everywhere constant at 45°, the equations become

$$P_x = P_o - \int_{x_o}^{x} (P-Q) \, dx \qquad 15$$

and

$$Q_x = Q_o - \int_{x_o}^{x} (P-Q) \, dx \qquad 16$$

The solution of these two equations amounts to evaluating the area under the (P-Q) curve to any point in question on the x axis and substituting this value for the value of the integral in either of the two equations. Since, at any point along an unloaded boundary, values of P and Q are known, it was then possible to determine either P or Q along the path of integra-

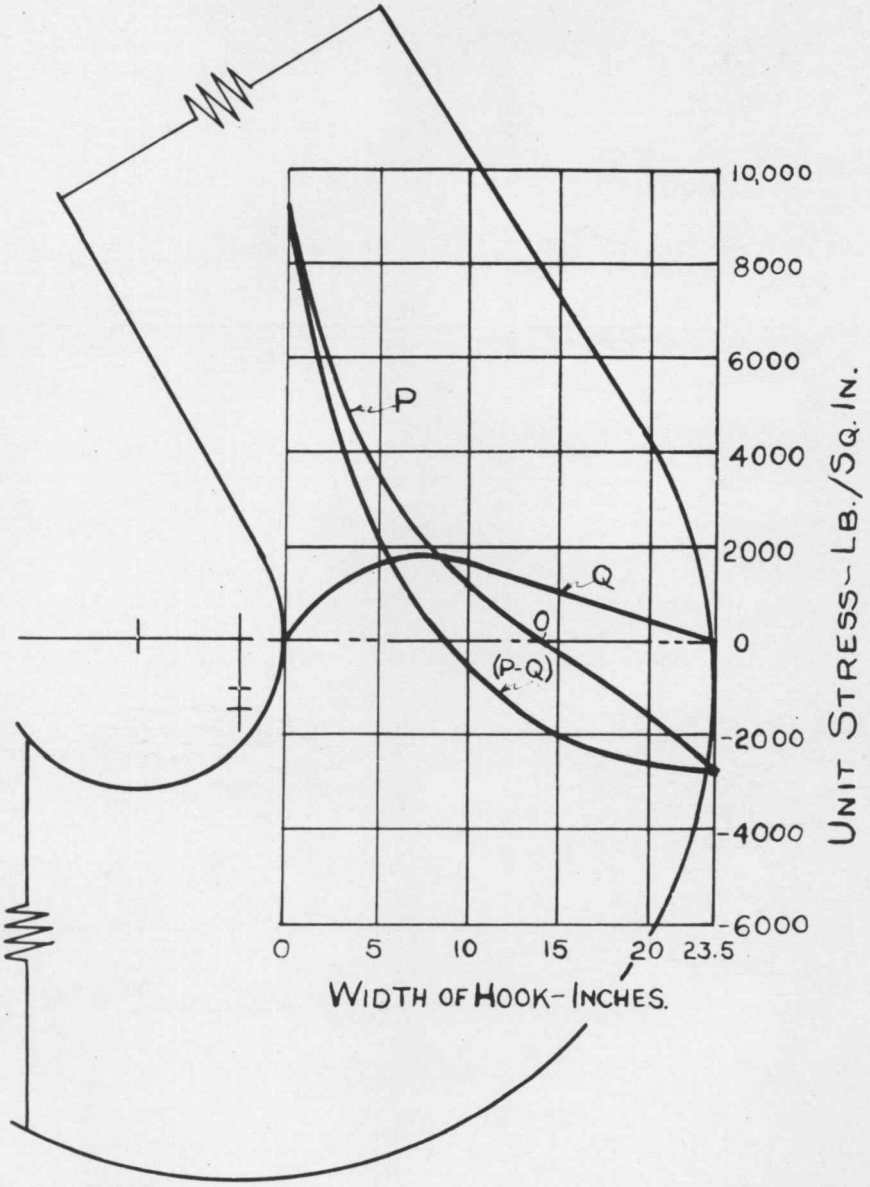

Fig.24.-Circumferential, Radial, and Maximum Shearing Stress through Critical Section of Plain Hook for Design Load. (125,000 Pounds).

gration. With the maximum value of the shearing stress and one of the principal stresses known for any point along the horizontal axis, the other principal stress could easilly be obtained. See Table III.

Fig.24 shows the values of the circumferential and radial stresses existing along the section of maximum moment for the case of the plain hook. It also shows that the point at which vertical stress is zero, and consequently the neutral axis, is located 14.25 inches from the point of maximum stress at the boundary. Also, the point at which the radial and circumferential stresses are equal, P = Q, the value of (P-Q) becomes zero. This point is an isotropic point, as previously stated.

As a check on the accuracy of the solution, a summation of the internal forces acting through their corresponding lever arms about the neutral axis, point O, should equal the external force multiplied by the distance through which it acts. The areas under both parts of the circumferential stress curve (P) were found from which the average stress ordinate for each part of the curve was obtained. The center of gravity for each part of the stress curve was also determined, thus locating the distance from the center of gravity of each part of the curve to the neutral axis on the point O. Knowing the area of the section acted on by

TABLE III

CIRCUMFERENTIAL AND RADIAL STRESSES FOR PLAIN PROTOTYPE HOOK IN PLANE OF MAXIMUM MOMENT WITH THE DESIGN LOAD

Distance on X axis from outer fiber	Maximum Shear at point X 1/2 (P-Q)	Radial Stress Q	Circumferential Stress P
Inches	Lb.per.sq.in.	Lb.per.sq.in.	Lb.per.sq.in.
0.00	4,725	0	9,450
0.22	4,600	141	9,350
0.60	4,100	350	8,560
0.97	3,587	550	7,710
1.50	3,070	775	6,940
2.02	2,562	980	6,100
2.70	2,050	1215	5,320
3.60	1,850	1430	4,510
4.80	1,025	1630	3,700
6.45	525	1800	2,820
8.55	0	1870	1,870
11.50	525	1770	750
18.00	1,025	1110	- 940
23.50	1,380	0	-2,760

Minus signs indicate compression.

the average ordinate, the equivalent internal force, in pounds, for each area was determined. Since the hook is in static equilibrium, the sum of the internal and external moments acting about any point must be equal to zero. For the particular case the results follow:

Taking a summation of moments about the point 0

$$-125{,}000 \text{ lb.} \times 22.25 \text{ in.} + 218{,}000 \text{ lb.} \times 10.80 \text{ in.} + 66{,}400 \text{ lb.} \times 5.95 \text{ in.} = 0$$

and 2,781,000 in.lb.= 2,360,000 in.lb.+ 395,000 in.lb. making 2,781,000 in.lb. = 2,745,000 in.lb. indicating that the calculated internal moment is equal to the external moment within a difference of approximately one percent.

It is obvious that a complete analysis of the total hook is possible by the same method, and that several sections through the model could be taken and the circumferential radial stresses determined from each. Also, for the two prototype hooks the same analysis might be made. From Figs.25 and 26 it is observed that the isoclinics are practically the same as for the plain model hook and for this reason any further results that would be obtained would be more or less of a repetition of those obtained from the reference design. In connection with Figs.25 and 26 it should be stated that the isoclinic lines were much wider than

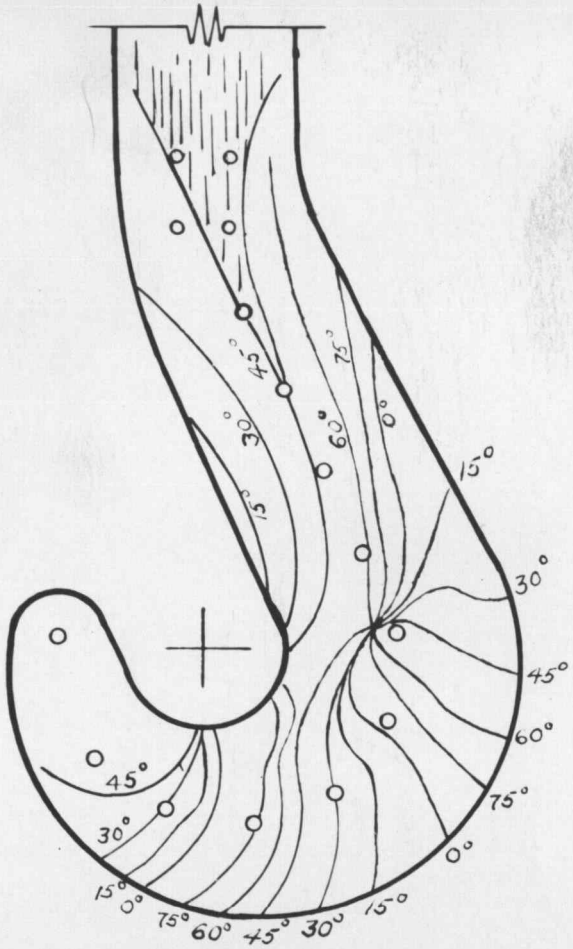

Fig.25.-Isoclinic Lines for Model of Design A.

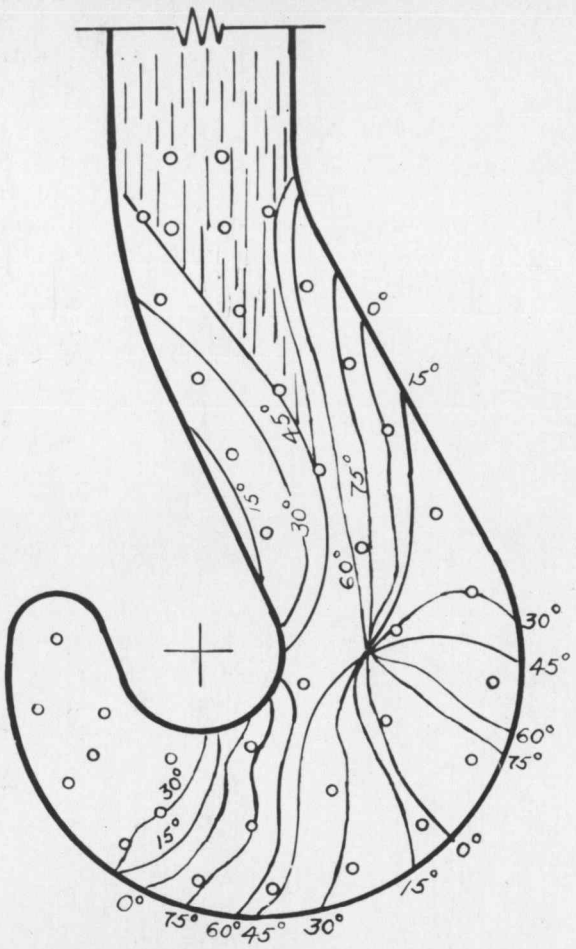

Fig.26.-Isoclinic Lines for Model of Design B.

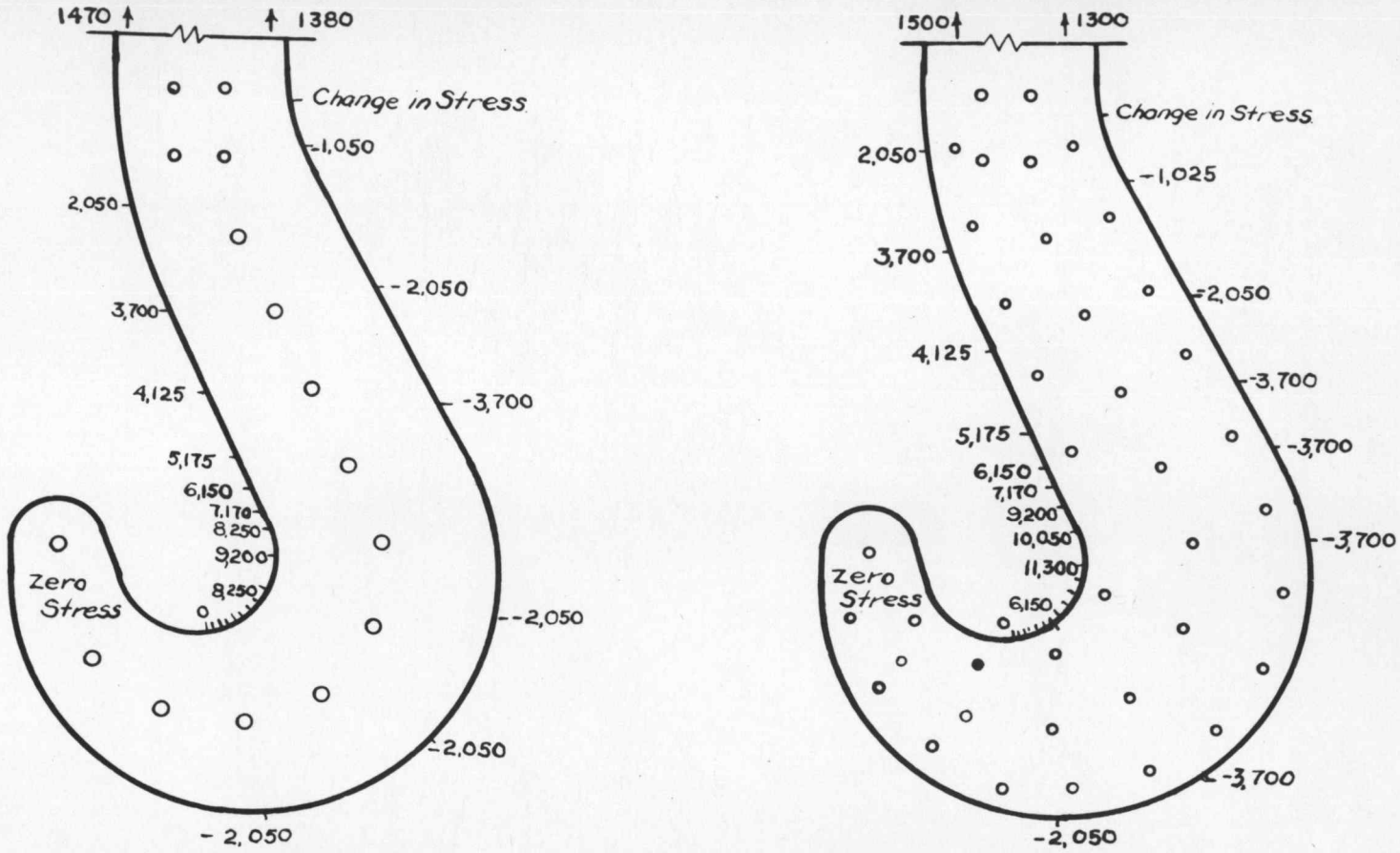

Fig.27.-Boundary Stresses in Lb.per sq.inch for Design Load
Scale-1"=19". (-) sign indicates compression.

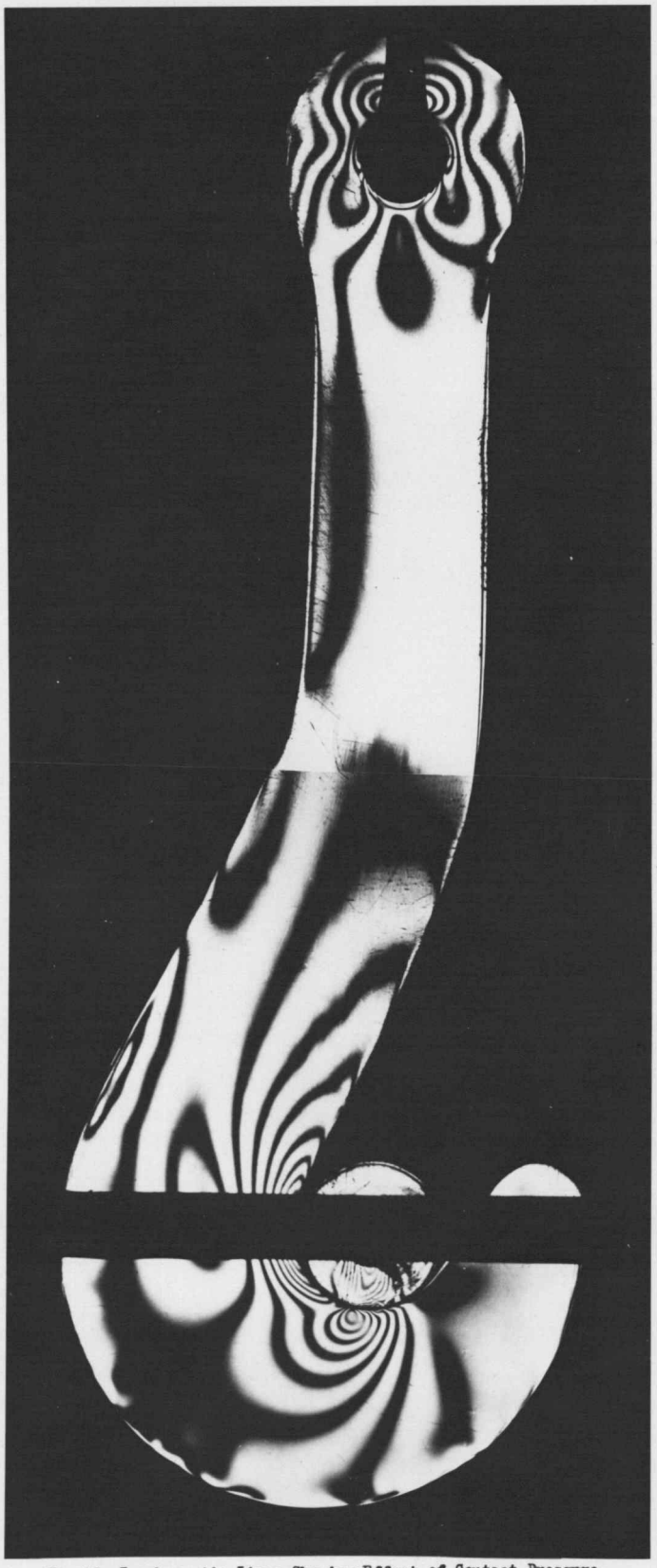

Fig.28.-Isochromatic Lines Showing Effect of Contact Pressure.

the diameters of the holes, and that it was impossible to determine their location in the direct vicinities of the holes. For an accurate analysis of the stresses around the rivet holes a model of much greater dimensions would have to be used and each rivet hole analysed as an individual area.

Fig.27 shows the magnitude of the boundary stresses existing at various points in the lower section of the prototype models at the design load, the values being obtained directly from the isoclinic lines. Values of stress between points can be obtained by direct interpolation. It is interesting to note that the "neck" of the hook is affected but very little from the bending stress as the tensile stress through the section is quite evenly distributed.

As a matter of interest, a jig was constructed so that an insight could be had as to the distribution of the stresses at the point of application of the load. Fig.28 shows the isochromatics at this point.

6. Results of Tests on Steel Models. As a correlation to the data obtained from photo-elastic investigations, the data obtained from the steel models tested was very encouraging. From the results in Table V, it is seen that the yield point for each of the models tested occurred at a load only slightly higher than the calculated load. This is only to be expected when

it is considered that the yield point, to produce noticeable strain, occurs at a stress slightly above the stress at the highest stressed fiber for this type of loading. As a matter of interest, the tests were continued on the steel hooks until what might be termed destruction occurred. The plain model, design C, and the model with the holes located in the geometric center, design A, exhibited no fracture but merely pulled out until the trunnion slipped over the end of the model. Design B, having the three concentric rivet lines, actually exhibited fiber failure, the failure progressing from the highest stressed section directly through to the rivet hole located slightly below the horizontal geometric axis of the hook opening. From these tests it was also noticed that the design of the neck and top of the hooks is such that no yield occurred at any point. See Fig.14.

Tables IV,V and VI show the results of all the tests performed, giving the data from the photo-elastic investigations in a condensed form.

TABLE IV

TESTS ON STEEL TENSILE SPECIMENS

Specimen No.	Original Cross Sect. Area	Yield Point.	Ultimate Strength	Breaking Load	Elong. in 2"	Percent Red. in area
	Sq.inch	#/sq.in.	#/sq.in.	#/sq.in	Percent	Percent
1	0.1405	33,000	57,400	41,600	35.0	66.2
2	0.1390	34,800	57,900	42,800	38.0	64.7

TABLE V

YIELD POINT DETERMINATION ON HOOK MODELS

Model Design No.	Scale of model to prototype	Calculated Load at Yield Pt. pounds	Actual Ld. at Yield Point. pounds	Maximum Load pounds	Type of Failure in final test
A	1:25	960	1040	3,670	Flow
B	1:25	795	870	3,390	Fracture
C	1:25	960	1090	3,710	Flow

Calculated load on basis of 34,000 lb./sq.in yield point.

TABLE VI

RESULTS FROM THE PHOTO-ELASTIC INVESTIGATION FOR THE THREE LADLE HOOK DESIGNS

Model Design	Scale Ratio to Prototype	Load on Model	Maximum fiber stress in model.	Maximum stress in prototype for design load.	Stress increase factor due to rivet holes.	Factor of safety-based on 30,000 lb. per sq.in.
		Pounds	Lb/sq.in.	Lb/sq.in.		
C	1:25	80	3,690	9,224		3.25
A	1:25	80	3,690	9,224	none	3.25
B	1:25	80	4,500	11,300	1.22	2.65

PART V

CONCLUSIONS

PART V. CONCLUSIONS

For purposes of studying the distribution of stress in models of rectangular cross section, where a direct condition of similarity exists between the model and the prototype, the photo-elastic method of analysis can be very successfully applied. In the particular investigation the highest stressed section of the hook occurred at an unloaded boundary, thus making it possible to determine the stress at that section from direct observations By a method of graphical integration, it was found possible to obtain a complete analysis of the circumferential and radial stresses existing throughout the entire hook models.

From an interpretation of the results obtained, it is apparent that for the design having the three rivet lines, referred to as design B, the rivet holes located in the section of maximum moment produce increased boundary stresses in that section. However, in the prototype model having a single row of holes located in the geometric axis of the hook, referred to as design A, no increase in stress is noted at the critical section over what is found in a similar model having no rivet holes at all. Also, since there are no marked stress concentrations at any point in the model of design A, its prototype would be recommended in preference to the prototype of design B. However, by eliminating the three

rivet holes nearest the boundary in the critical section from the latter design, the maximum stress resulting from equal loads on any of the models tested would be nearly identical.

Referring to the specifications for ladle hook design, page 15-section 41-paragraph 21, the code reads- "Where two hooks or a pair of hooks are used, these shall preferably be laminated steel plate hooks, the plates securely riveted together. The hooks may be forged from a solid billet of steel. They shall be designed so as to have a factor of safety of 6 as a minimum on the elastic limit capacity of the hooks". From the results of this investigation, the maximum fiber stress in the plain hook and in the single rivet line design was found to be 9,224 lb.per.sq. inch for the design load of 62.5 tons. The corresponding stress in the design using three lines of rivets was 11,300 lb.per sq. in. The specifications for the steel from which the hooks are manufactured call for a yield point of 30,000 lb.per sq.in., giving corresponding factors of safety of 3.25 and 2.65 respectively. On the basis of the code as stated, neither of the submitted designs passes the specifications. However, on page 23 under note 6, dealing with formulas for the design of hooks, a value of 12,000 lb.per sq.in. is specified as the maximum unit stress allowable for ladle hooks. All of the

designs analyzed meet this requirement.

For a complete analysis of the sfresses existing at the rivet holes, much larger models than used in this investigation would have to be used and each rivet hole analyzed as a separate area. However, in this investigation, interest was directed more on the effect of the rivet holes on the maximum fiber stress existing and hence the effect on the ultimate performance of the hooks rather than on the magnitude of the stress concentrations at the holes. Although it was found, by direct observation, that the stress concentrations at the holes in the three rivet line design were greater than those in the single rivet line design, the magnitude of these concentrations is at no point allarming. A stress increase factor of 1.22 was found in the prototype of design B over design A, these being due to the effect of three rivet holes located in the critical section.

The Winkler-Bach equation, as commonly applied to curve beam analysis and design gives a factor of safety of 1.12 over the maximum fiber stress existing in a ladle hook having the same dimensions as the prototypes but having no rivet holes. Therefore, if special attention is given to the effect of the rivet holes, this equation is quite applicable to the design of ladle hooks similar to the ones investigated here.

PART VI

APPENDIX

BIBLIOGRAPHY

1. Baud, R. V. On the Determination of Principal Stresses from Crossed Nicol Observations. Jour.Franklin Inst.,211:457-474,1931

2. Baud, R. V. and Wright, W.D. The Analysis of the Colors observed in Photo-elastic Experiments. Jour.Opt.Soc. of Am.,20:381-395,1930

3. Beyer, A. H. and Solakian, A.G. Photo-elastic Analysis of Stresses in Composite Materials. Trans.A.S.C.E.,98:1064-1070,1933.

4. Brahtz,H.G.A. Practical Method for Determination of Stresses at Two-dimensional Sharp and Rounded Corners of Elastic Structures. Report to the Bureau of Reclamation, U.S.Dept. of Interior.

5. Coker, E. G. and Filon, L.N.G. Treatise on Photoelasticity University Press, Cambridge, Eng., 1932. Complete Bibliography to 1930 included.

6. Eberhart, H. D. Photoelastic Analysis Of a Pier Section of the Bonneville Dam. Thesis submitted to Oregon State College. June-1935.

7. Filon, L. N. G. On the Graphical Determination of Stress from Photo-elastic Observations. Engineering(London)511-512,Oct.19,1923

8. Frocht, M. M. Recent Advances in Photo-elasticity. Trans. A.S.M.E. APM 54-9:83-96. 1932.

9. Frocht, M. M. On the Application of Interference Fringes to Stress Analysis Jour.Franklin Inst.,216:73-89.1933.

10. Heymans, P. Photo-elasticity and its Application to Engineering Problems. Tech.Engr.News,3:3,80-85.June 1922.

11. Love, A. E. H. Mathematical Theory of Elasticity. Cambridge University Press, 2nd Edition, 1906.

12. McGivern, J. G. and Supper, H. L. A. A Membrane Analogy supplementing Photo-elasticity. Trans. A.S.M.E.,56:601-607,1934.

13. Minarik, R. G. Stress Analysis by the Photo-elastic Method. Univ. of Cal.Press, March 1934.

14. Morley, Arthur Engineering--vol.98.p321.

15. Neuber, Heins P.Exact construction of the (P+Q) Network from Photo-elastic Observations. Trans.A.S.M.E.,56:733-739,1934.

16. Seely, F. B. Advanced Mechanics of Materials 108-114,191-208. 1932.

17. Solakian, A. G. New Developments in Photo-elasticity. Jour. Opt.Soc.of Am.22:293-306,May 1932.

18. Stone, M. Construction of (P+Q) Lines. Trans.A.S.M.E.,APM 54-10:115-116.1932.

19. Timoshenko, S. Theory of Elasticity. McGraw-Hill, Monographs. 123-134;168.,1934.

20. Timoshenko, S. Strength of Materials. D.Van Nostrand Part II. 423-473. 1930

21. Wahl, A. M. and Beeuwhes, R. Jr., Stress Concentrations produced by Holes and Notches. Trans. A.S.M.E.,56:617-627,1934.

22. Winslow, A. M. and Edmonds, R. H. G., Tests and Theory of Curved Beams. Trans. A.S.M.E.48:647-678. 1926.